1.0

1.1

1.25   1.4   1.6

2.8   2.5

2.2

2.0

1.8

AD A111709

②

UNSTEADY WALL-PRESSURE

MEASUREMENTS FOR UNDEREXPANDED

NOZZLES EXHAUSTING INTO LAUNCH TUBES

Stanley A. Bouslog,

Ed J. Zihlman, Jr.,

and

John J. Bertin

U.S. ARMY MISSILE COMMAND
Redstone Arsenal, Alabama 35898

DTIC
ELECTE
MAR 5 1982
S D

B

DTIC FILE COPY

SMI FORM 1021, 1 JUL 79 PREVIOUS EDITION IS OBSOLETE

82 02

REPORT DOCUMENTATION PAGE		READ INSTRUCTIONS BEFORE COMPLETING FORM
1. REPORT NUMBER TR-RL-CR-82-1	2. GOVT ACCESSION NO. AD - 111 709	3. RECIPIENT'S CATALOG NUMBER
4. TITLE *(and Subtitle)* Unsteady Wall-Pressure Measurements for Underexpanded Nozzles Exhausting Into Launch Tubes		5. TYPE OF REPORT & PERIOD COVERED Contractor Report
		6. PERFORMING ORG. REPORT NUMBER Fluid Dynamics Inst. 81-105
7. AUTHOR(*s*) Stanley A. Bouslog, Ed. J. Zihlman, Jr., and John J. Bertin		8. CONTRACT OR GRANT NUMBER(*s*) DAAH01-80-C-0118 DAAH01-81-C-B078
9. PERFORMING ORGANIZATION NAME AND ADDRESS Department of Aerospace Engineering and Engineering Mechanics UT-Austin, Austin, TX 78712		10. PROGRAM ELEMENT, PROJECT, TASK AREA & WORK UNIT NUMBERS
11. CONTROLLING OFFICE NAME AND ADDRESS		12. REPORT DATE Jan. 1982
		13. NUMBER OF PAGES
14. MONITORING AGENCY NAME & ADDRESS*(If different from Controlling Office)*		15. SECURITY CLASS. *(of this report)* UNCLASSIFIED
		15a. DECLASSIFICATION/DOWNGRADING SCHEDULE

16. DISTRIBUTION STATEMENT *(of this Report)*

Approved for public release; distribution unlimited.

17. DISTRIBUTION STATEMENT *(of the abstract entered in Block 20, if different from Report)*

18. SUPPLEMENTARY NOTES

19. KEY WORDS *(Continue on reverse side if necessary and identify by block number)*

Launch-tube flow fields, viscous/inviscid interactions, rocket-exhaust flows.

20. ABSTRACT *(Continue on reverse side if necessary and identify by block number)*

An experimental program has been conducted to measure the unsteady pressures acting on the launcher wall due to an underexpanded nozzle exhausting into a constructive launcher. The data exhibited a transient behavior similar to that observed in flight tests.

DD $_{1\ JAN\ 73}^{FORM}$ 1473   EDITION OF 1 NOV 65 IS OBSOLETE

BLANK PAGE

CONTENTS

FIGURES

FIGURES (Cont'd)

FIGURES (Cont'd)

DELIBERATELY BLANK

1. (U) INTRODUCTION

The designer of a tube-launched rocket system must consider the flow field inside the launch tube as the rocket is launched. Unless the annular gap between the rocket and the launch tube is sealed by a ring (e.g., an obturator ring), viscous interactions associated with the expansion of the exhaust flow as it leaves the nozzle and the subsequent impingement of the exhaust on the launcher wall will produce a "secondary" flow in the annular gap. Barnette et al.[1] have shown that the trajectory of a tube-launched rocket can be significantly affected by the unbalanced forces associated with this secondary flow. To predict the magnitude and the direction of the flow in the annular gap, one must be able to describe the exhaust plume of the rocket and the viscous/shock interaction structure that results when the plume encounters the launcher wall. The strength of the impingement shock-wave and the characteristics of the viscous interaction at the wall depend on the structure of the exhaust plume and on the geometry of the launch tube. When an under-expanded, supersonic nozzle exhausts into a constant-area tube, the strength of the impingement shock wave depends on the Mach number of the inviscid flow along the inner edge of the mixing zone at the plume boundary, on the velocity profile in the mixing zone, on the ratio of the specific heats (γ), and on the inclination of the impinging flow relative to the launcher wall.

However, many launch tubes are such that their cross-section area does not remain constant. The presence of rails, frangible bore riders, and changes in the cross-section serve as constrictions to the exhaust flow. Constrictions located in the exhaust flow downstream of the nozzle can produce dramatic changes in the launch-tube flow field. If the reduction in cross-section area due to the constriction is relatively large, the constriction (or the constrictive section) may serve as a second throat, choking the exhaust flow in the launch tube. Thus, the mass-flow-rate that can pass through the constriction is limited and additional exhaust gases must flow upstream into the annular gap between the rocket and the launcher wall, i.e., significant blow-by flow occurs. For these flows, a strong shock wave is generated when the plume impinges on

---

[1] D. W. Barnette, J. J. Bertin, and J. L. Batson, "Free-Flight Rocket's Initial Trajectory as Affected by Massive Blow-by", Journal of Spacecraft and Rockets, Vol. 15, No. 6, Nov.-Dec. 1978, pp. 334-340.

the wall, producing a large pressure gradient that turns a significant fraction of the flow upstream into the annular gap. Choking of the exhaust flow by a constrictive change in cross-section has been observed both in cold-gas tests at the University of Texas at Austin[1] and in flight tests at the White Sands Missile Range[2].

If the reduction in cross-section area due to the constriction is not sufficient to choke the flow in the launch tube, a complex system of reflecting shock waves will be established. For these flows, the impingement shock wave is weak and the pressure rise across the impingement shock is such that it is possible that (1) the exhaust flow entrains air from the annular gap and the system acts as an ejector or that (2) a relatively small fraction of the exhaust flow is turned upstream into the annular gap, i.e., relatively weak blow-by flow occurs. However, because the constriction contains forward-facing surfaces, the blow-by flow rate depends on the distance from the nozzle-exit-plane, as well as those parameters mentioned in the first paragraph.

The blow-by flow rate for unchoked flow was determined as a function of the nozzle-exit-plane location relative to the front of a constrictive ring[3]. Based on the experimentally-determined mass-flow-rates and static wall-pressure distributions, four characteristic flow-fields were observed. (1) When the nozzle-exit-plane is very close to the ring, i.e., $\tilde{x}_{ne} \leq 2.0h$, the exhaust plume does not encounter the front face of the ring and no blow-by flow occurs. (2) With the nozzle exit-plane located between 2.0h and 3.0h upstream of the ring, a portion of the exhaust flow impinges directly on the front face of the ring and "splashes" back,

[1] D. W. Barnette, J. J. Bertin, and J. L. Batson, "Free-Flight Rocket's Initial Trajectory as Affected by Massive Blow-by", Journal of Spacecraft and Rockets, Vol. 15, No. 6, Nov.-Dec. 1978, pp. 334-340.

[2] ———— : "Feasibility Flight Testing of Rocket Impelled Projectile (RIP)", Report Number 7-52100/3R-5, 1 May 1973, LTV Aerospace Corporation, Michigan Division.

[3] S. A. Bouslog and J. J. Bertin, "Flows in the Annular Region When an Underexpanded Nozzle is exhausted into a Stepped Launch Tube", U.S. Army Missile Command, TR RL-CR-80-4, Redstone Arsenal, Alabama, March 1980.

generating relatively large secondary flow-rates *upstream into the*
annular gap. A sketch of this blow-by flow pattern is presented in
Figure 1a. (3) With the rocket placed further upstream, the exhaust
flow impinges on the launcher wall ahead of the ring. Due to the
close proximity of the ring, the impingement process is affected by
the presence of the step. A sketch of the flow field that results
when the nozzle-exit-plane is located in this intermediate region,
i.e., $3.0h \leq \tilde{x}_{ne} < 10.0h$, is presented in Figure 1b. Significant
blow-by flow can occur when the nozzle-exit-plane is in this region.
(4) When the exhaust plume impinges on the wall sufficiently far
from the ring (or step), a flow field similar to that for a forward-
facing step in a supersonic flow is established, e.g. [4], as shown
in the sketch of Figure 1c. *Wall-pressure measurements just upstream*
of the step[3] exhibit a pressure plateau and a local peak-pressure
typical of a forward-facing-step pressure distribution. The ring
becomes isolated for $\tilde{x}_{ne} > 10.0h$ and the blow-by flow rates are
essentially those for a constant-area tube.

The data presented in ref. 3 are time-averaged values. An
additional experimental program has been conducted using transducers
capable of measuring the unsteady pressures acting on the launcher
wall for a nozzle-exit-location of 8.0h. At this position, the
exhaust flow impinges on the launcher wall upstream of the ring but
close enough to the ring to generate significant blow-by flow. One
pressure-transducer was used to measure the unsteady pressures in
the region between the nozzle-exit-plane and the impingement loca-
tion, while the other transducer was used to record the unsteady
pressure in the annular gap. The unsteady pressures for several
orifice locations are presented in this report over a range of
stagnation pressures from 2.77×10^6 N/m^2 (400psi) to 8.96×10^6
N/m^2 (1300psi).

[3] S. A. Bouslog and J. J. Bertin, "Flows in the Annular Region
When an Underexpanded Nozzle is exhausted into a Stepped Launch
Tube", U.S. Army Missile Command, TR RL-CR-80-4, Redstone Arsenal,
Alabama, March 1980.

[4] D. R. Chapman, D. M. Kuehn, and H. K. Larson, "Investigation of
Separated Flows in Supersonic and Subsonic Streams with Emphasis
on the Effects of Transition", Report 1356, 1957, NACA.
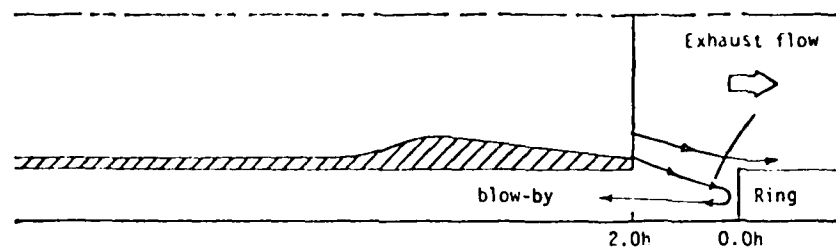
(a) Splash-back of exhaust flow into annular gap, $\tilde{x}_{ne} = 2.0h$.
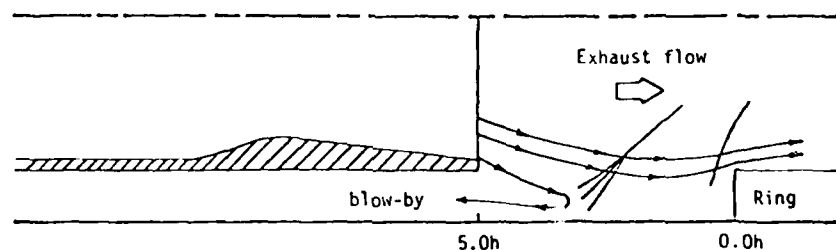
(b) Exhaust flow impinges on launcher wall ahead of ring,
$3.0h \le \tilde{x}_{ne} < 10.0h$.
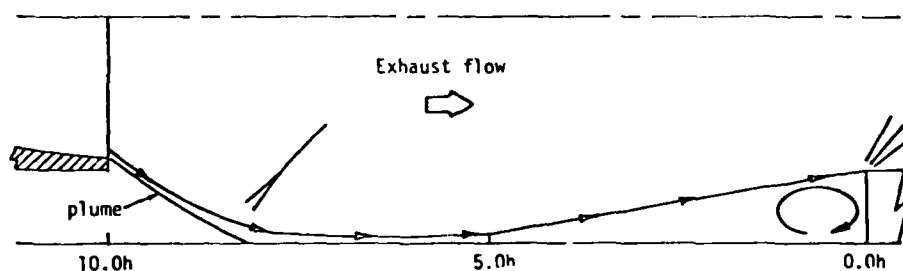
(c) Sketch of plume impinging on wall, creating an
"isolated" forward-facing step.

$x_{ne} > 10.0h$

Figure 1. - Sketches of flow fields for a nozzle exhausting
upstream of a constrictive ring in a launch tube.

2. EXPERIMENTAL PROGRAM

2.1 Test Facility

The tests were conducted at the Rocket Exhaust Effects
Facility located at the Experimental Aerodynamics Laboratory (EAL)
of the University of Texas at Austin. A schematic diagram of this
blow-down type facility is presented in Figure 2. Simulated rocket
exhaust plumes were obtained by accelerating unheated, compressed
air (the test gas) through a pipe with a convergent-divergent nozzle
(the simulated rocket). The simulated rocket (i.e., the pipe/nozzle
configuration) was threaded to a high pressure supply line and held
firmly in place by a yoke assembly. The simulated launch tube was
mounted on a moveable table. By moving the table in the x (or
streamwise) direction, the location of the launch tube relative to
the exit plane of the simulated rocket nozzle could be varied.

2.2 Simulated Rocket

A sketch illustrating the geometry of the $10°$ conical con-
vergent-divergent nozzle used to produce the simulated rocket exhaust
is presented in Figure 3. The nozzle-exit radius, r_{ne}, is 1.237 cm
(0.487 in.). The area ratio of the nozzle, A_{ne}/A^*, is 2.316. If
one assumed isentropic gas flow relations, the nozzle-exit-plane
Mach number is 2.36. Experimentally determined pitot pressures in
the nozzle-exit of this nozzle indicate that the nozzle-exit-plane
Mach number is between 2.32 and 2.39[5]. Despite the existence of
internal shock waves, (which originate in the vicinity of the throat),
the isentropic gas flow relations closely predict the nozzle-exit-
plane Mach number.

2.3 Simulated Launch Tube

As shown in Figure 4, the L1 launch tube[3] has an internal
radius of 1.20 r_{ne}. During most of the test program, a ring was
placed in the launch tube downstream of the rocket. The height of
the ring was equal to the radial dimension of the annular gap be-
tween the rocket and the launcher wall (see Figure 5). The

[3] S. A. Bouslog and J. J. Bertin, "Flows in the Annular Region
When an Underexpanded Nozzle is exhausted into a Stepped Launch
Tube", U.S. Army Missile Command, TR RL-CR-80-4, Redstone Arsenal,
Alabama, March 1980.

[5] S. J. Sutter, J. J. Bertin, D. P. Dannemiller, and E. J. Zihlman, Jr.,
"Study of the Exhaust Plume for Highly Underexpanded Supersonic
Nozzles Exhausting into Quiescent Air", Aerospace Engineering
Report 79001, January 1979, University of Texas at Austin.
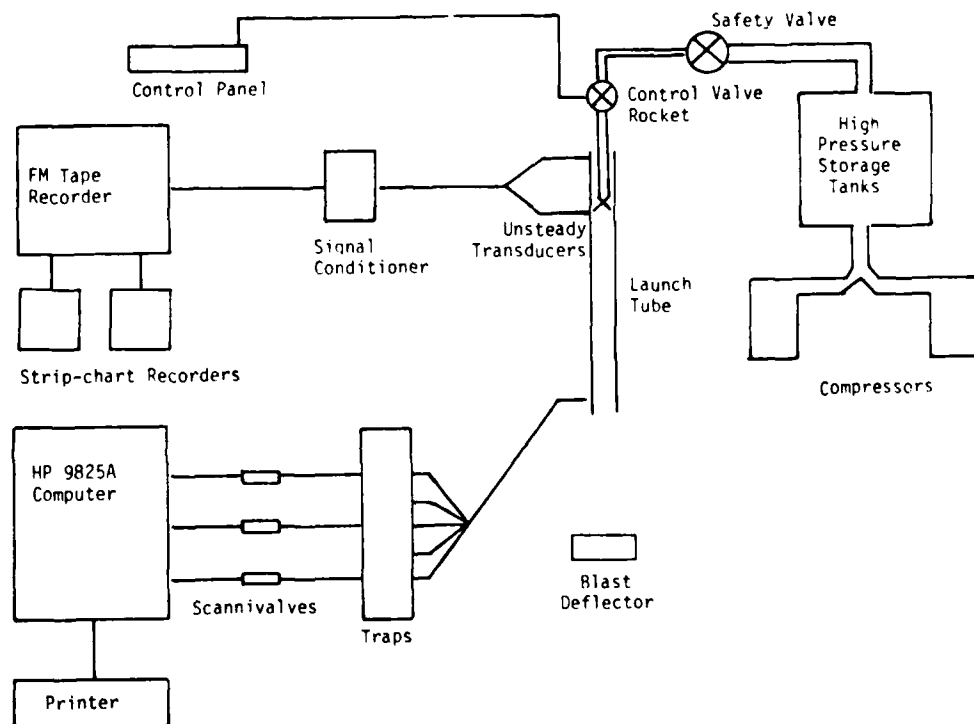
Figure 2. - Schematic of the University of Texas Exhaust Effects Facility.

Equations for Divergent Section (cm):

For $-2.479 \leq x \leq -2.338$

$(x + 2.479)^2 + (r - 1.626)^2 = (0.813)^2$

For $-2.338 < x \leq 0.0$

$r = 0.176 \, x + 1.237$

$r^* = 0.813$
(0.320)

0.813
(0.320)

$\theta_{ne} = 10°$

1.080
(0.425)

$x = -2.479$
(0.976)

$r_{ne} = 1.237$
(0.487)

$r_r = 1.334$
(0.525)

r_{ne}

$x = 0.0$

Figure 3. – 10° Conical Nozzle, i.e., the C4 Nozzle.

13

Note: All dimensions in centimeters (inches).
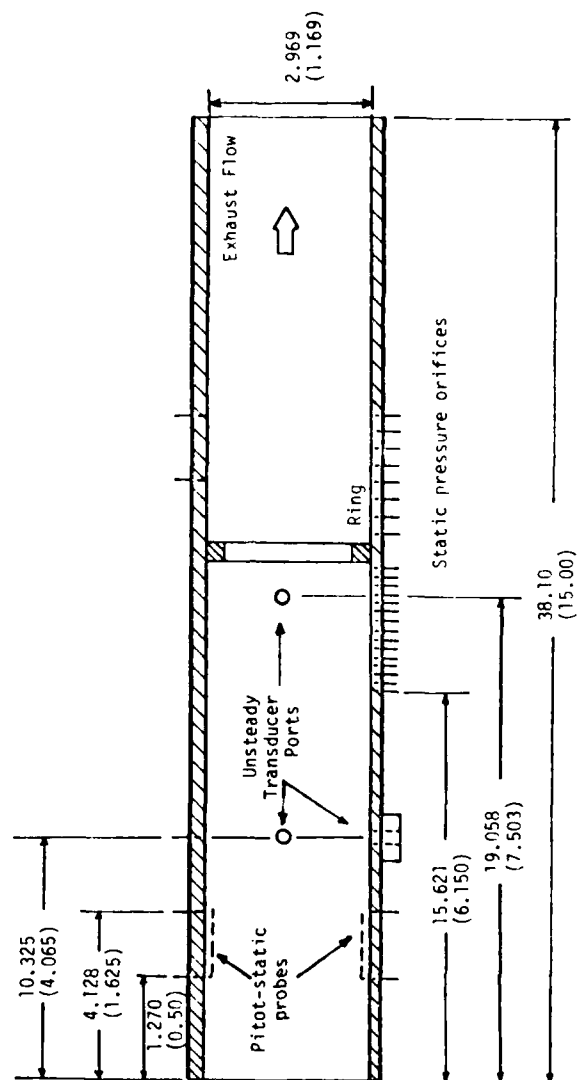
Figure 4. - Instrumentation of the L1 Launch Tube with Constrictive Ring.

14
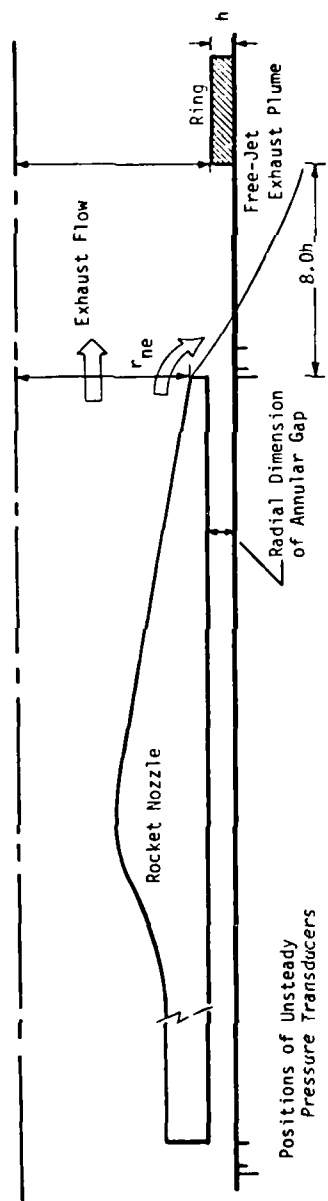
Figure 5. - Positions of Unsteady Pressure Transducers Relative to the Nozzle-exit Plane.

15

instrumentation in the tube consisted of static-pressure orifices in the launcher wall, a pitot-static system, and three positions for mounting two unsteady pressure transducers. The static-pressure orifices were used to obtain time-averaged measurements of the static pressures inside the tube. As shown in the sketch of Figure 4, these orifices were located axially along the tube wall, upstream of the ring at a spacing of 0.25 r_{ne} (0.309 cm.). Additional static pressure orifices spaced 0.50 r_{ne} (0.613 cm.) apart were located downstream of the ring. The pitot-static system, located near the forward end of the launcher in the annular gap, was used to measure the mass flow-rate in the annular gap. Also, three ports were added to the L1 launch tube so that two transducers could simultaneously measure the unsteady pressures both in the impingement region and in the annular gap. It should be noted that each unsteady transducer mount wa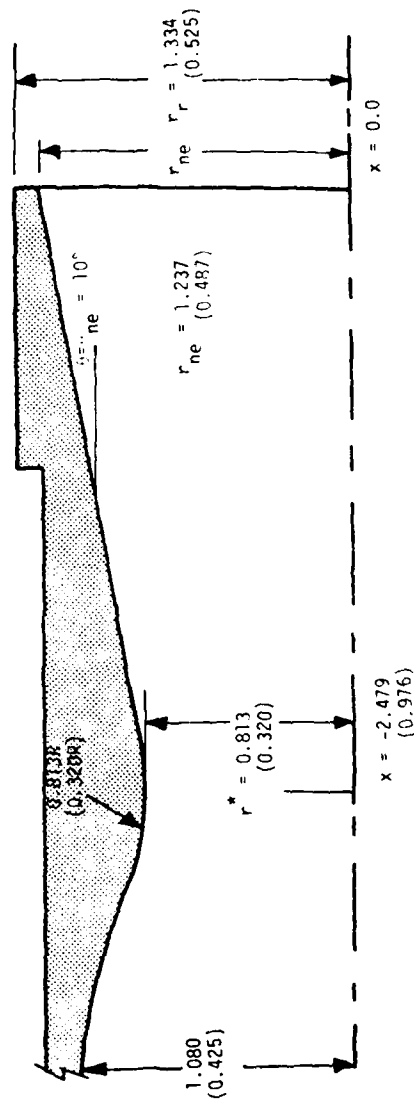s located in the same axial plane as a static-pressure orifice but were in different angular planes. Thus, although the unsteady pressures could be compared to the time-averaged pressures at the same axial position, the comparisons would be affected by asymmetries inherent in the flow.

2.4 Coordinate Systems

For this test program two axial coordinate systems were used. The non-dimensional coordinate x/r_{ne} was used in measuring the position of pressure taps and transducer mounts relative to the nozzle-exit-plane, such that positions downstream of the nozzle-exit-plane were positive. The non-dimensionalized coordinate $\bar{x}/h$, where h is the height of the ring, was used in measuring the distance from the front face of the ring, such that positions upstream of the ring were positive. These two coordinate systems are illustrated in Figure 6.

2.5 Data Acquisition

To monitor the static-pressures and the mass flow-rates in the launch tube, a data acquisition system consisting of a set of pressure traps, a scannivalve system, and a HP9825 mini-computer were used. Photographs and a detailed description of this system are available[6]. Output from the mini-computer included the non-

---

[6] E. S. Idar, III, J. J. Bertin, and S. Bouslog, "The Effect of Geometry on Static Wall-Pressure Distributions and Secondary Flows for Tube-Launched Rocket Configurations", Aerospace Engineering Report 79005, November 1979, The University of Texas at Austin.
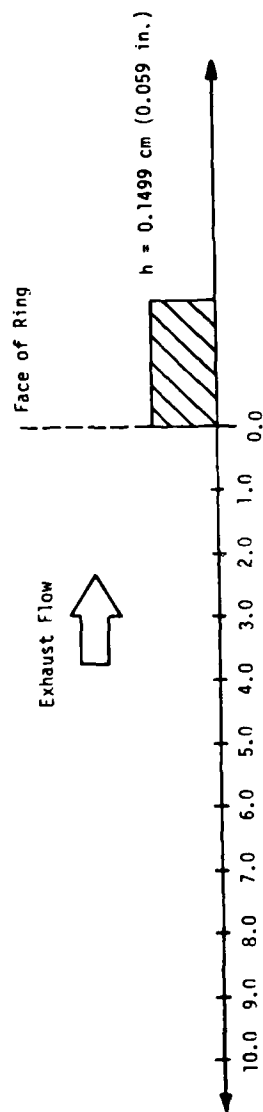
(a) $\tilde{x}/h$ - coordinate system, distances relative to the ring.
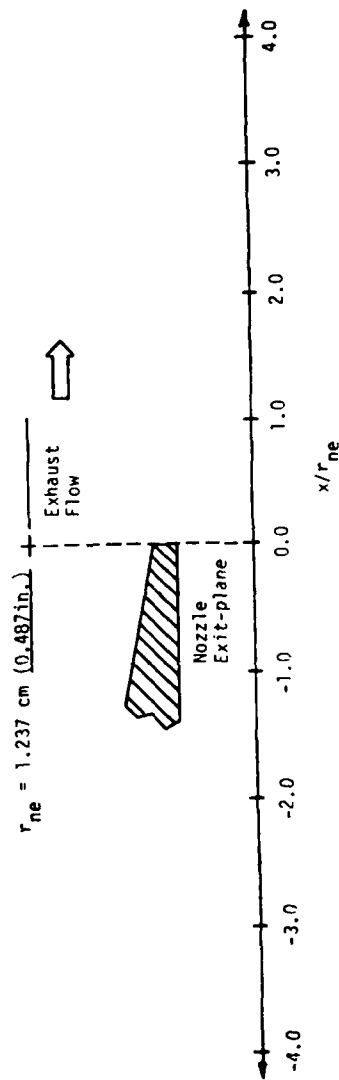
(b) x/r_{ne} - coordinate system, distances relative to the nozzle exit-plane.

Figure 6. - Coordinate Systems for Present Test Program.

17

dimensionalized static-pressures acting on the launcher wall, (p/p_{t1}), the nozzle stagnation pressure, and the pitot-probe pressures. Comparisons of these data with data obtained from previous tests with this rocket nozzle/launch tube configuration, C4/L1, provided a means to monitor the flow field that existed in the tube.

In order to measure the unsteady pressures of the flow field inside the launch tube, two Endevco Model 8506 piezo-resistive full-bridge pressure transducers were used. These transducers have a 15 psig range with high frequency response and low sensitivity shift ($\pm$ 4% of Full Scale output). Even though these characteristics are not appreciably affected by relatively low temperatures, the rapid expansion of the supersonic jet of unheated air produced icing on the wall of the launch tube in close proximity to the flush mounted transducer. To alleviate this problem the transducer that was located near the impingement location was recessed into the wall of the launcher and sensed pressures through a 0.064 cm. (0.025 in.) hole. Recessing the transducer prevented an ice build-up on the protective screen of the transducer, but it probably diminished the transient response of the transducer. Nevertheless, the data obtained with the recessed transducer compared much better with the average pressure measured at the static-pressure orifice in the same plane.

Once the transducers were in position co-axial cables were used to connect them to a signal conditioner and then to a FM tape recorder. Both during and after the run the output could be viewed on a strip chart recorder or on an oscilloscope. The data presented in this report are copies of the strip chart traces in which the static pressures appear as a function of time.

2.6 Test Program

The test apparatus and data acquisition equipment used at the Rocket Exhaust Effects Facility required the following steps be taken in order to conduct the experiments. First, the launch tube was firmly attached to the table and aligned with the simulated rocket nozzle, so that their axes were collinear. Then, the constrictive ring was positioned inside the tube. By using three different widths of rings the relative position between the nozzle-exit-plane and the front face of the ring could be maintained, while changing the relative position of the unsteady pressure transducers (Figure 5). For the first set of runs, the ring was 0.618 cm (0.244 in.) wide. With the nozzle-exit-plane positioned at $\bar{x} = 8h$, or eight ring heights upstream from the ring, one unsteady pressure transducer was located in the base region, directly under the nozzle-exit $x_g = 0.0 \, r_{ne}$. Data were taken at nozzle stagnation

18

pressures ranging from 8.96 x 10^6 N/m^2 (1300 psia) to 2.77 x 10^6 N/m^2 (400 psia).

A wider ring, 0.942 cm (0.371 in.) wide, was then placed on the launch-tube wall. The rocket nozzle was again positioned $\tilde{x}$ = 8h from the ring. By using a wider ring, the unsteady pressure transducer was located nearer the exhaust impingement, x_g = 0.04 r_{ne}. Again, data were taken at stagnation pressures ranging from 8.96 x 10^6 N/m^2 (1300 psia) to 2.77 x 10^6 N/m^2 (400 psia).

For the third set of runs a still wider ring, 1.189 cm. (0.468 in.), was used, so that the unsteady transducer was located nearer still to the impingement region, x_g = 0.13 r_{ne}. Data were obtained for the same stagnation pressures.

It should be noted that during all runs the upstream unsteady transducer was located well into the annular gap. Therefore, the pressures measured by this transducer should be approximately the same for each stagnation pressure, regardless of the ring width.

DELIBERATELY BLANK

3. DISCUSSION OF RESULTS

An experimental program has been conducted in which unheated air was exhausted from an underexpanded nozzle into a launch tube fitted with a constrictive ring (or step). In a previous investigation of this configuration[3], time-averaged values of the static wall-pressures, of the static pressures on the surface of the rocket, and of the pitot pressures in the annular gap were obtained. Based on the data presented in reference 3, it was concluded that the reduction in area due to the presence of the ring was not sufficient to choke the flow in the tube. Nevertheless, it was clear that the presence of the ring modifies the impingement process and can cause significant blow-by flow rates. The blow-by flow was found to be a function of the nozzle-exit-plane location relative to the face of the ring and of the stagnation pressure. Although the exhaust flow impinges on the launcher wall well ahead of the ring when the nozzle-exit-plane is located such that $3.0h \leq \bar{x}_{ne} \leq 10.0h$, the presence of the ring modifies the impingement process. Thus, the data discussed in this report are for the nozzle in this region.

3.1 Repeatability of the Time-Averaged Pressures

The time-averaged values of the static pressure for the launch-tube wall for $\bar{x}_{ne} = 8.0h$ as measured during the previous test program and during the present program are presented in Figure 7. The time-averaged values are presented for two different stagnation pressures. Since the measurements from the two programs are consistent, the conclusions about the flow field that were determined from the data of the previous program should be valid for these tests.

Mass flow-rate data for the annular gap of the C4/L1 configuration (as taken from ref. 3) are presented in Figure 8. In order to measure the mass flow-rate in the annular gap, two pitot-probes were positioned diametrically apart, midway between the launcher wall and the rocket. The reader is cautioned that the pitot-pressure measurements for this particular nozzle/launch-tube configuration are of questionable accuracy due to the fact that the pitot probe was large relative to the width of the annular gap. Nevertheless, the trends of the data can give meaningful conclusions. Referring to Figure 8, one can see that, when the rocket nozzle is 8.0h from the forward face of the ring, significant blow-by occurs

---

[3] S. A. Bouslog and J. J. Bertin, "Flows in the Annular Region When an Underexpanded Nozzle is exhausted into a Stepped Launch Tube", U.S. Army Missile Command, TR RL-CR-80-4, Redstone Arsenal, Alabama, March 1980.
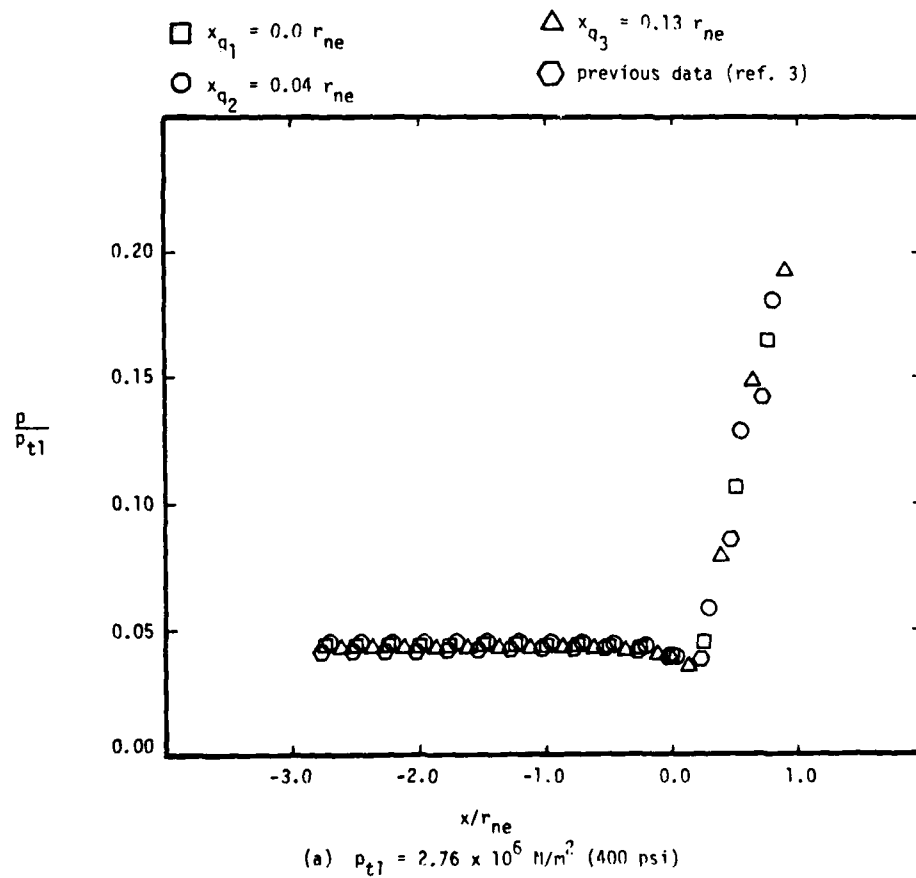
Figure 7. - The Repeatability of Static-wall Pressures for $\tilde{x}_{ne}$ = 8.0h.

The plot legend reads:

$\square$ x_{q_1} = 0.0 r_{ne} $\triangle$ x_{q_3} = 0.13 r_{ne}

$\bigcirc$ x_{q_2} = 0.04 r_{ne} $\hexagon$ previous data (ref. 3)

Y-axis: $\dfrac{p}{p_{t1}}$ with values 0.00, 0.05, 0.10, 0.15, 0.20

X-axis: x/r_{ne} with values -3.0, -2.0, -1.0, 0.0, 1.0

(a) p_{t1} = 2.76 x 10^6 N/m^2 (400 psi)

22
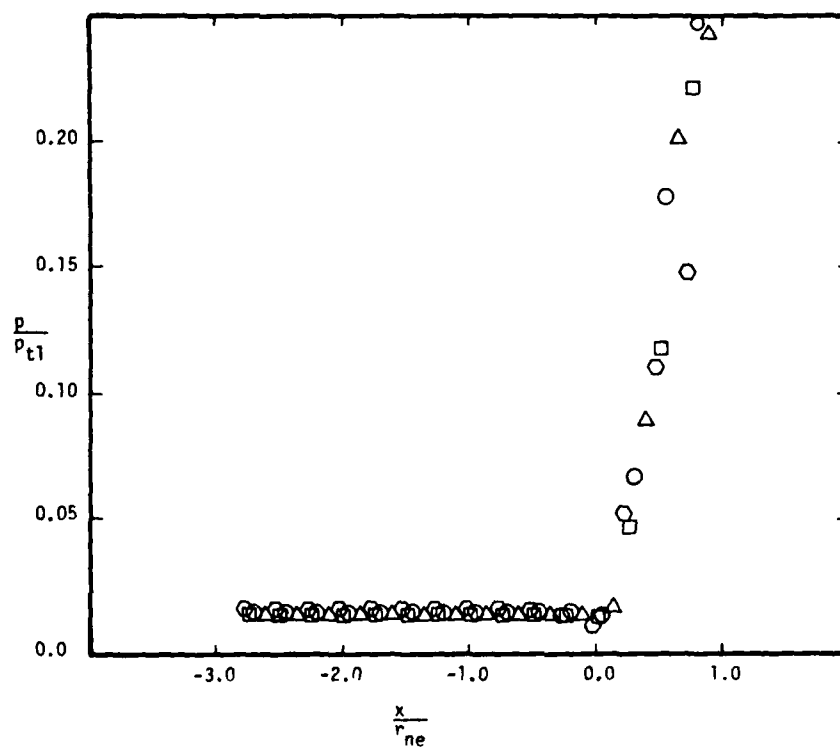
(b) $p_{t1} = 8.96 \times 10^6$ N/m^2 (1300psi)

Figure 7. - Concluded.

Figure 8. - Non-dimensional mass flow-rate in the annular
gap as a function of the nozzle exit-plane
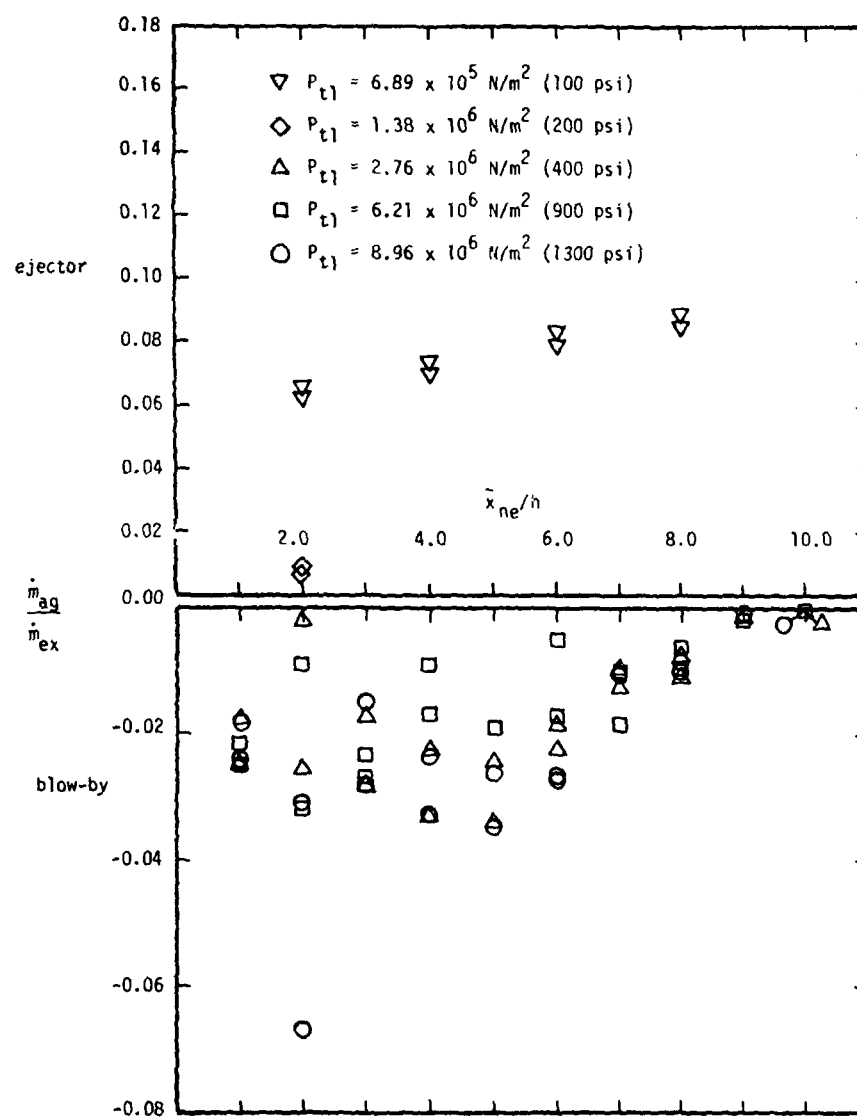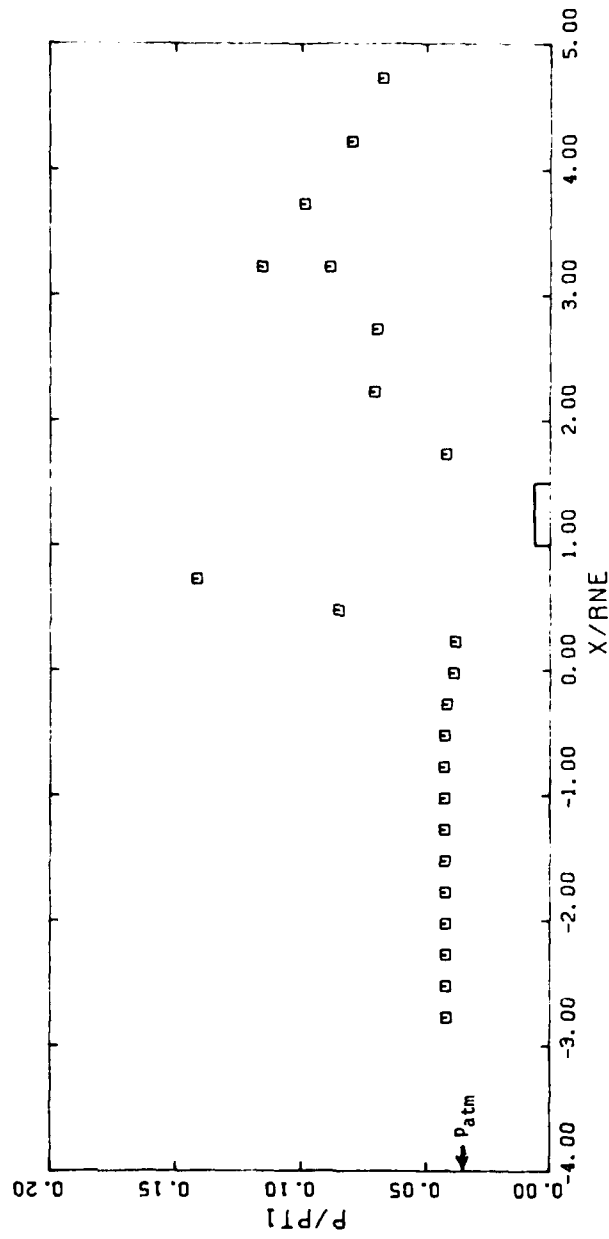position. Data for the C4/L1 configuration.

24

for stagnation pressures of 2.76×10^6 N/m^2, or greater. This observation based on the pressure measurements was confirmed by the use of tufts placed on the rocket. The mass flow-rate data indicate that an ejector flow exists for all nozzle positions when the stagnation pressure is 1.38×10^6 N/m^2, or less.

The steady-state static-wall-pressure distributions for $\tilde{x}_{ne} = 8.0h$ as taken from ref. 3 are reproduced in Figure 9. Note that, although there is a rapid rise in the static wall-pressures in the impingement region, there is no pressure plateau between the impingement of the exhaust flow on the wall and the face of the ring (or step). As noted in ref. 4 and in the Introduction, the absence of a pressure plateau indicates that the step was not isolated for this nozzle-exit location. It is of interest to examine carefully the pressure measurements for $0.00 \; r_{ne} \leq x \leq 1.00 \; r_{ne}$, since the orifice locations from Figures 10-12 are located in this region. Note that the wall pressure is a minimum just prior to the plume impingement. Thus, even though a portion of the flow from the shear layer at the plume boundary is turned upstream and flows along the wall (as blow-by flow), the wall pressure is apparently dominated by the entrainment action (ejector-type flow) at the plume boundary, away from the wall. Note that in this complex flow pattern, the blow-by (exhaust) gases at the wall move in the opposite direction to the exhaust gases in the plume. Furthermore, the location of the pressure minimum is just upstream of the impingement, i.e., in a location where the plume boundary is relatively near the wall. Note also that plume impingement is further downstream for the lower stagnation pressures. Thus, for $p_{t1} = 400$ psia, the wall pressure at $x = 0.00 \; r_{ne}$ is actually greater than that at a point further downstream. This will be evident in the transient data presented in Figures 10a and 11a.

Because of the relatively large blow-by flow rates, the pressures in the annular gap are higher than the atmospheric value. This will also be evident in the transient data, as will be discussed in Figures 13 through 15.

3.2 Pressure Histories

The histories of the static wall-pressure measurements for the orifice located in the impingement region are presented in Figure 10 through Figure 12. The data presented in Figure 10 were obtained with the transducer located in the plane of the nozzle exit, i.e., $x_g = 0.00 \; r_{ne}$. The gage was located at $0.04 \; r_{ne}$ and at $0.13 \; r_{ne}$ downstream of the nozzle exit plane for the tests of Figure 11 and of Figure 12, respectively. Recall that the locations of these orifices were presented in Figure 5. The data for the gage that was located well upstream in the annular gap are presented in Figure 13 through Figure 15. Before examining the data in detail, let us review some general characteristics of the flow.
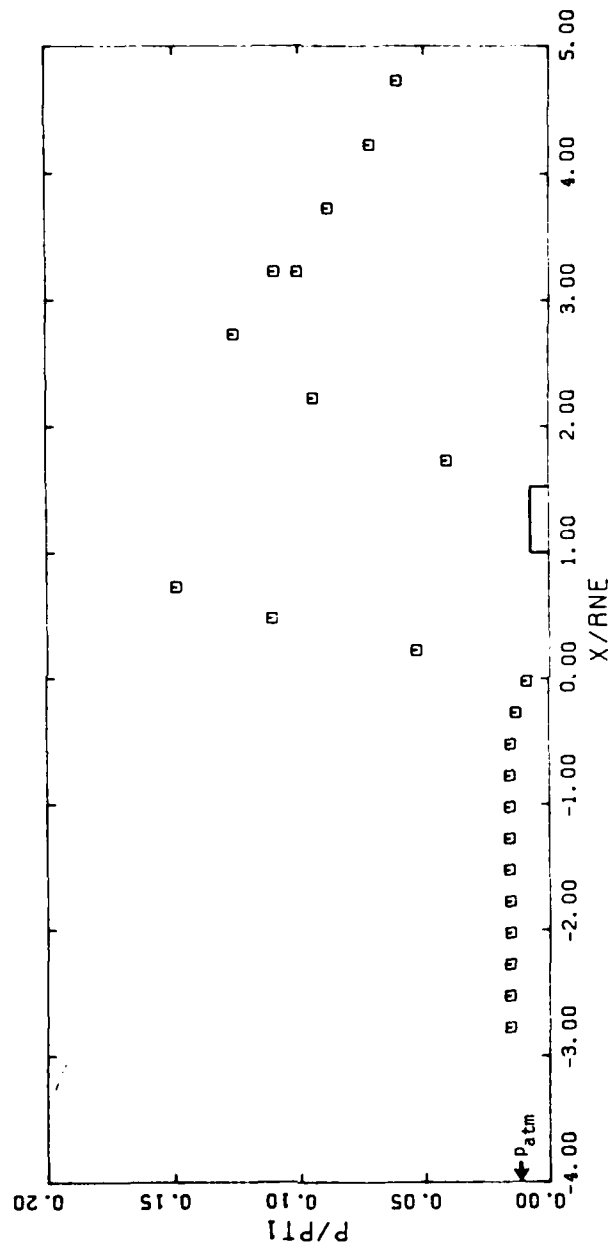
25

Figure 9. - The static wall-pressure distribution for the C4/L1 configuration with constrictive ring, $\tilde{x}_{ne}$ = 8.0h (ref. 3).

(a) PT1 = 400.00 psi (2.76 x 10^6 N/m^2)
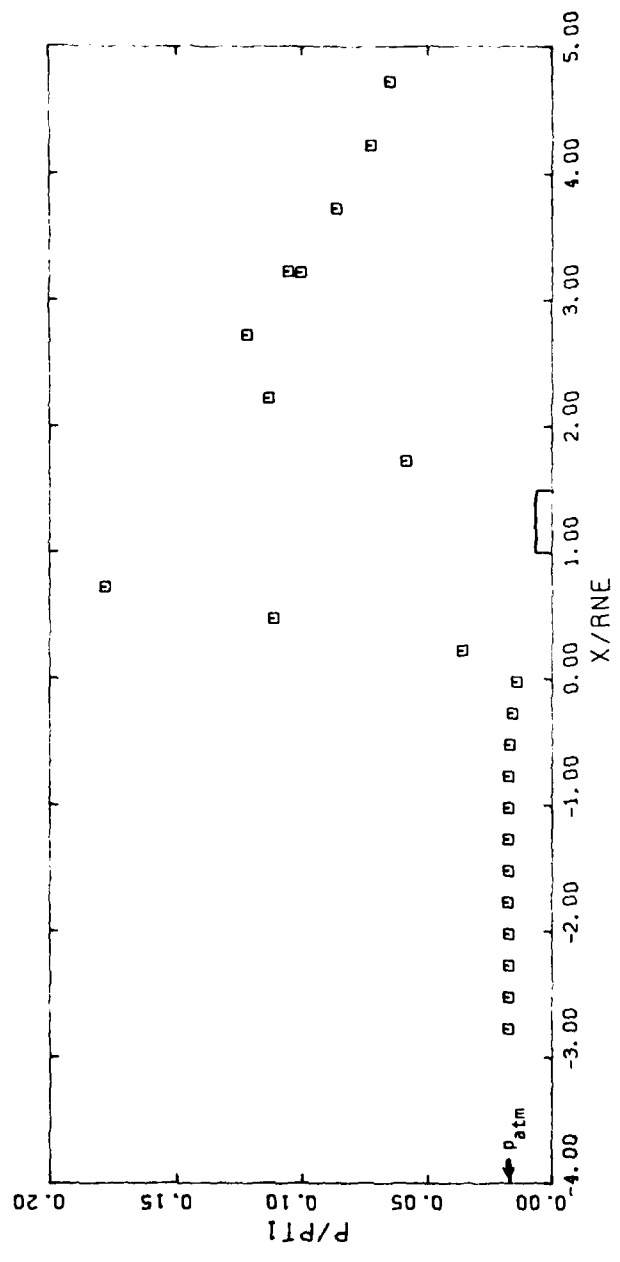
(b) $PTj = 900.00$ psi $(6.1 \times 10^6$ N/m$^2)$

Figure 9. – Continued.

27

(c) PT1 = 1300.00 psi (8.96 × 10^6 N/m^2)

Figure 9. – Concluded.

28

3.2.1 Characteristics of the flow

The simulated rocket exhaust is of several seconds duration with the exhaust air being released through the supply chamber/nozzle assembly from the external storage tanks by means of a rapidly opening valve. The test is terminated by closing the valve. Thus, the stagnation pressure increases from the atmospheric value to the test value in approximately two seconds at the beginning of the test. The stagnation pressure returns to the atmospheric value during the shutdown process, which is of similar duration. Extremely low pressures are measured on the launch tube wall as the stagnation pressure builds up during the initial phase and as it decreases during the terminal phase of the test. The low pressures result because the system acts as an ejector at the low stagnation pressures. The strong ejector action produced during the start up and the shutdown processes is evident in all of the pressure histories presented in Figures 10 through 15.

As can be seen in the data of Figures 10 through 12, the low pressure associated with the ejector action was followed by a transient overshoot before reaching the "steady-state" value for the particular test conditions. It is believed that this transient behavior occurs as the flow tries to expand from the nozzle to the temporarily, relatively-low base pressures creating a rather strong impingement shock wave. The resultant pressure rise across the impinging shock interacts with the base pressure causing it to increase, which would act to reduce the turning angle and, therefore, decrease the strength of the impingement shock wave. The process is complicated by the fact that the stagnation pressure is increasing simultaneously. Since the "overshoot" precedes the high negative ejector pressures during the shutdown process, the process appears to be a complex interplay between the rapidly changing stagnation pressure and the viscous interaction of the impingement process.

3.2.2 Transient pressures

Let us discuss first the data of Figures 10 and 11. The steady-state value of the static wall-pressure for $x_g = 0.00$ r_{ne} and for $x_g = 0.04$ r_{ne} decreases with stagnation pressure for $p_{t1} < 1089$ psia. As was noted when discussing the data of Figure 9, the entrainment process at the plume boundary appears to be a dominant factor in the wall pressures in this region. Thus, for $p_{t1} < 1089$ psia, the wall static pressure is greatest for the lowest value of the stagnation pressure (i.e., $p_{t1} = 393$ psia). For $p_{t1} \geq 1089$ psia, the rapid increase in the pressure in this region begins to reflect the impingement of the plume's snear layer. This is evident in the "time-averaged" values presented in Figure 9 and in the transient peaks which occur during midtest at the highest pressure of Figure 10c and the two higher pressures of Figure 11c.
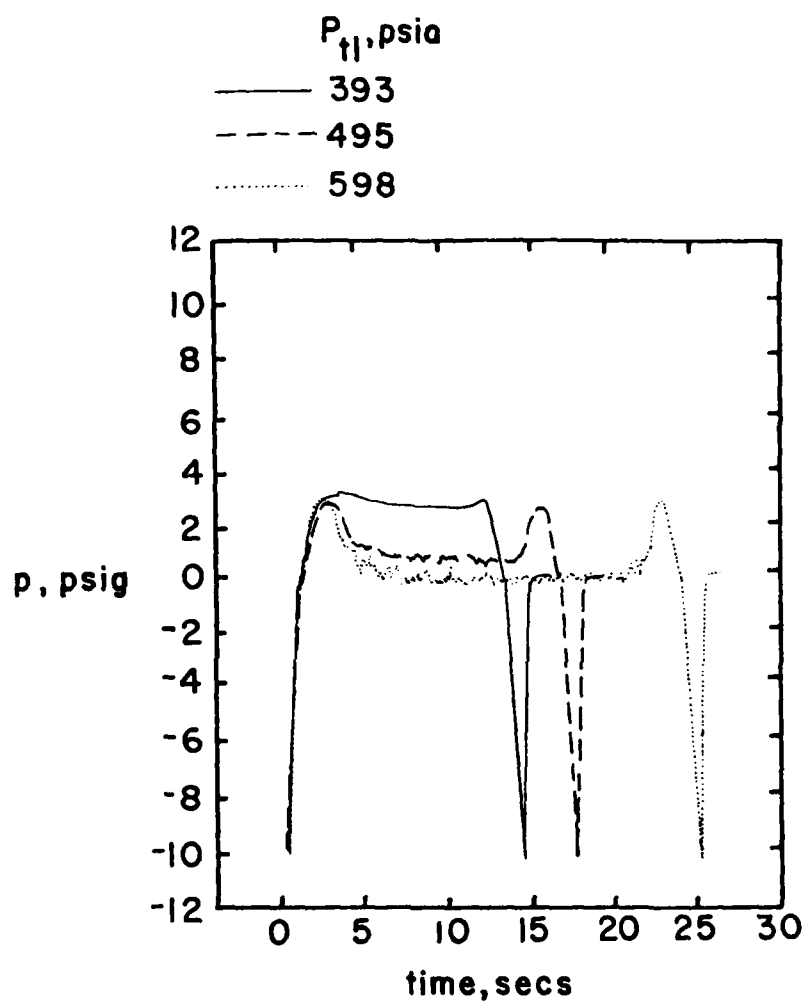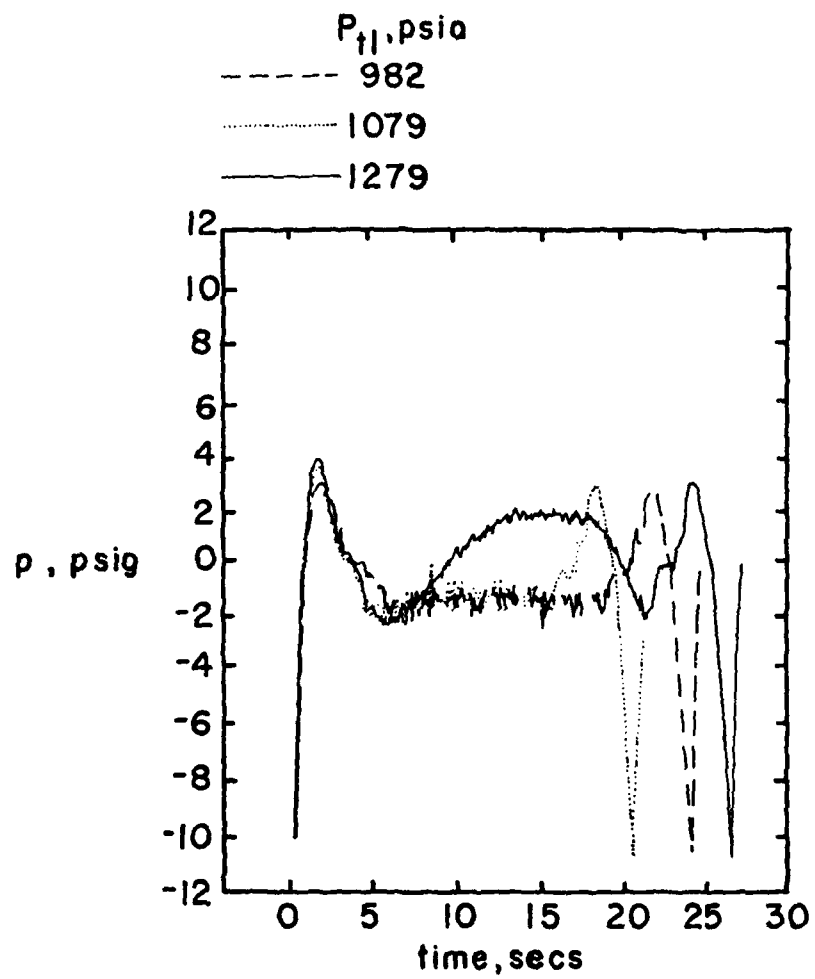
(a) Relatively low stagnation pressures.

Figure 10. - Static wall-pressure measurements from the
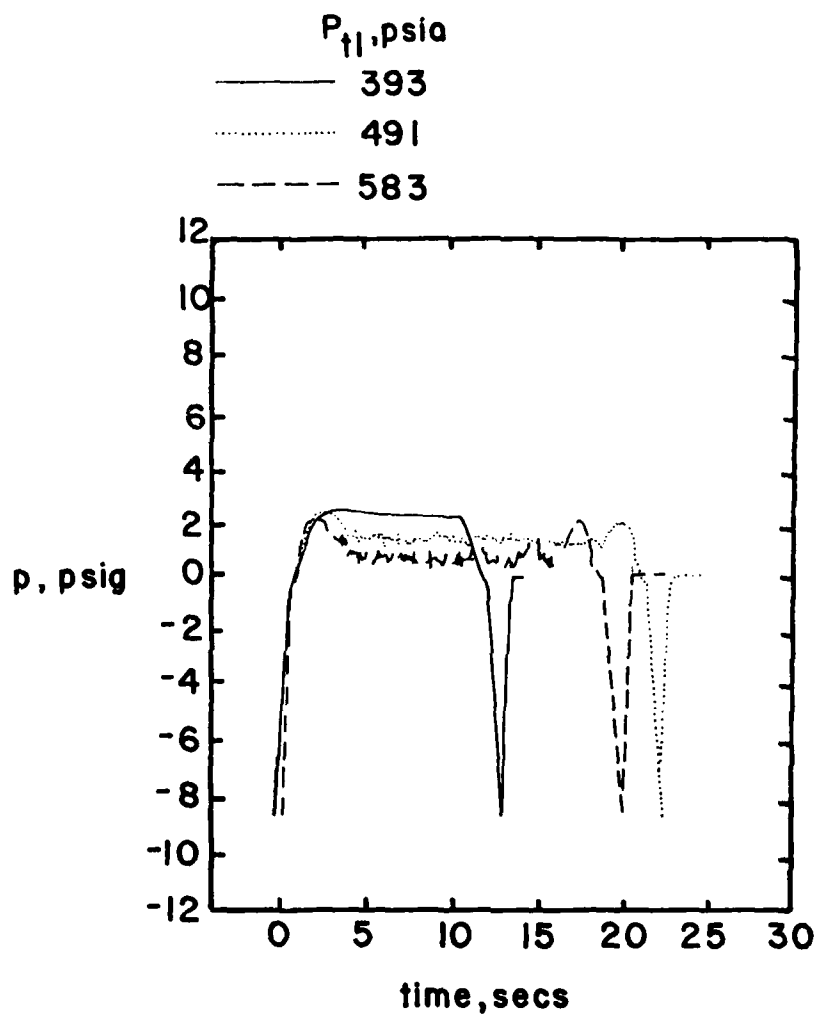impingement region, $x_g = 0.00\ r_{ne}$.

P_{t1},psia
—— 710
- - - 792
······ 894
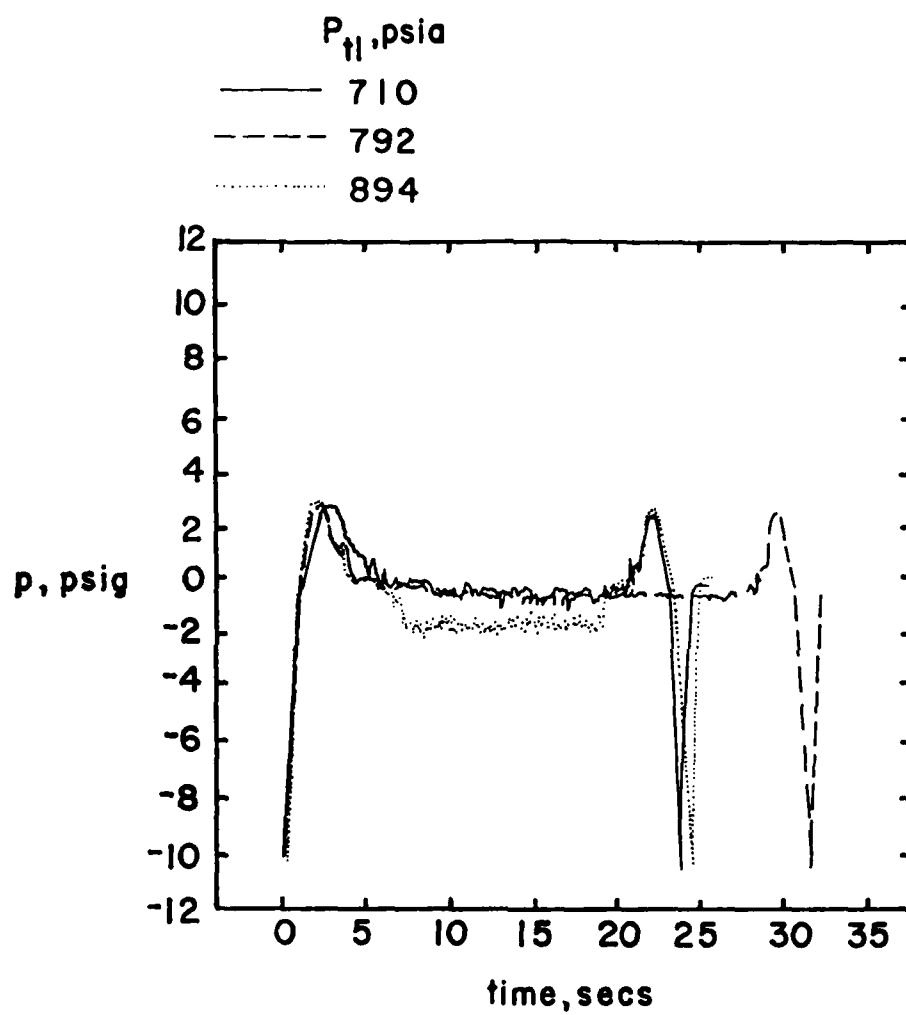
(b) Mid-range stagnation pressures.

Figure 10. - Continued.

31

(c) Relatively high stagnation pressures.

Figure 10. - Concluded.

32

P_{tl}, psia

—————— 393

················ 491

— — — 583

p, psig

time, secs

(a) Relatively low stagnation pressures.

Figure 11. - Static wall-pressure measurements from the impingement region, $x_g = 0.04\ r_{ne}$.

33

(b) Mid-range stagnation pressures.
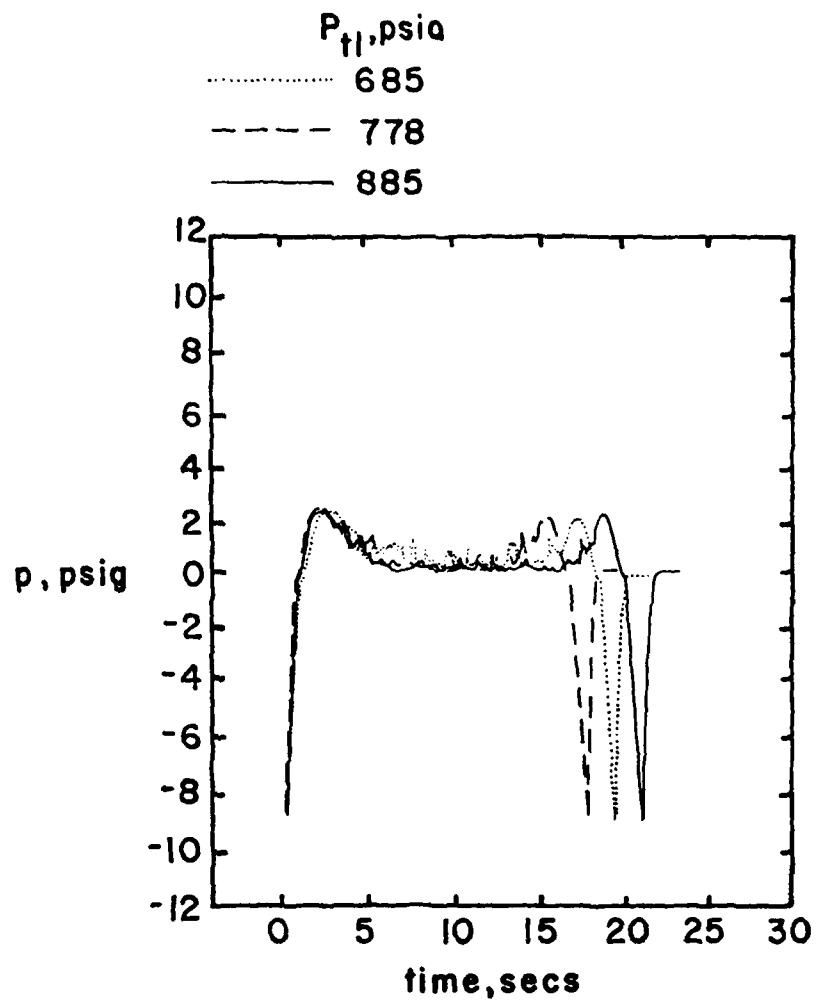
Figure 11. - Continued.

34

(c) Relatively high stagnation pressures.
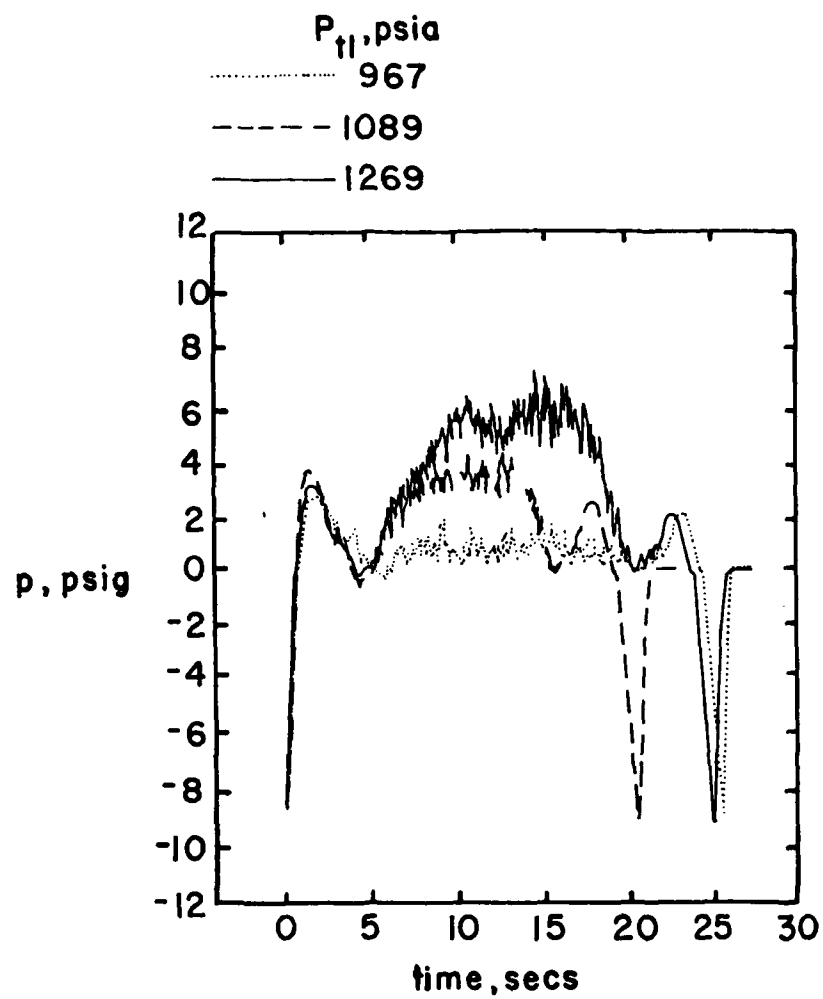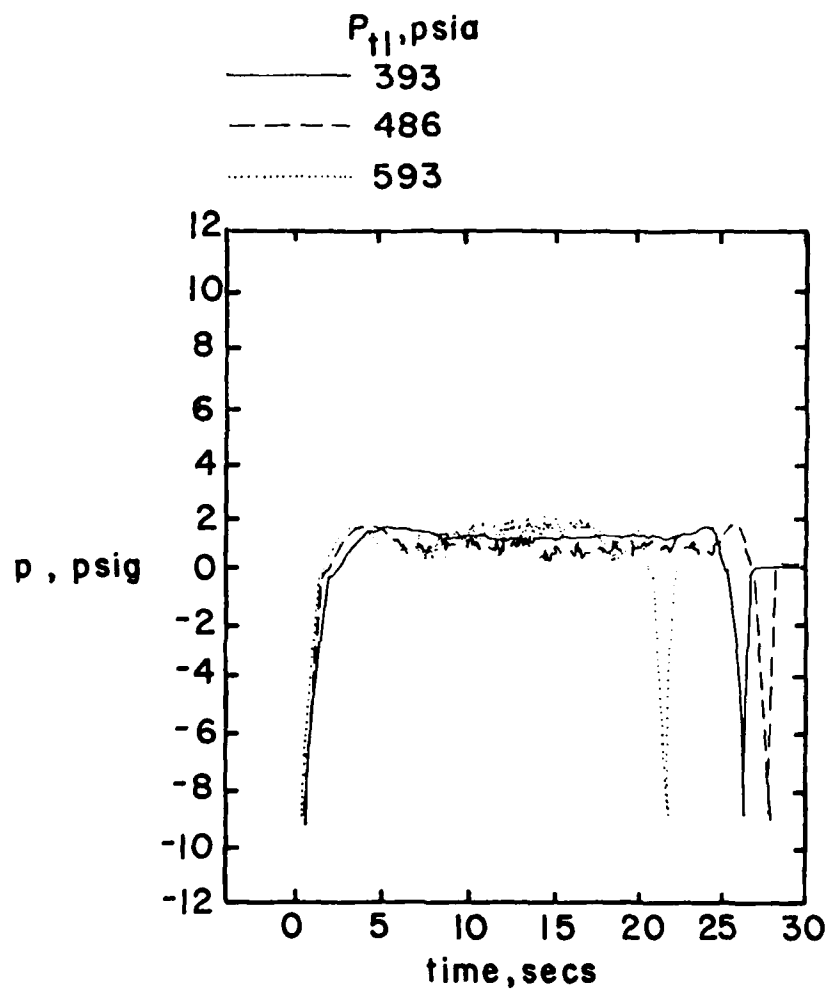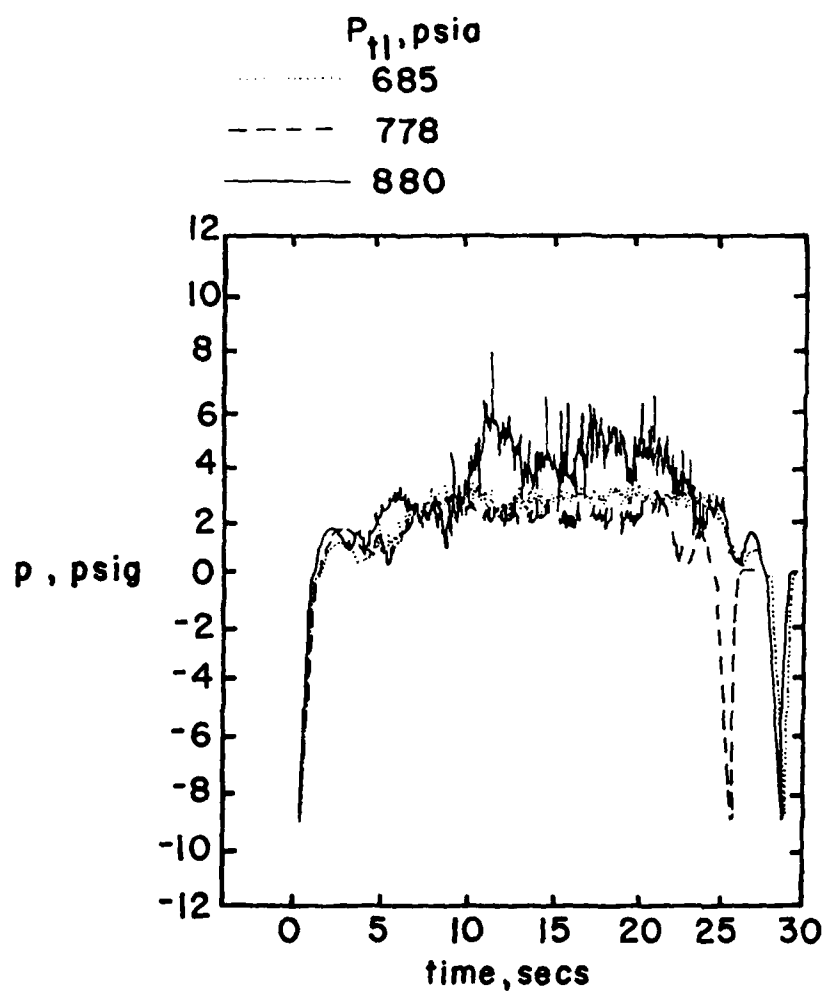
Figure 11. - Concluded.

(a) Relatively low stagnation pressures.
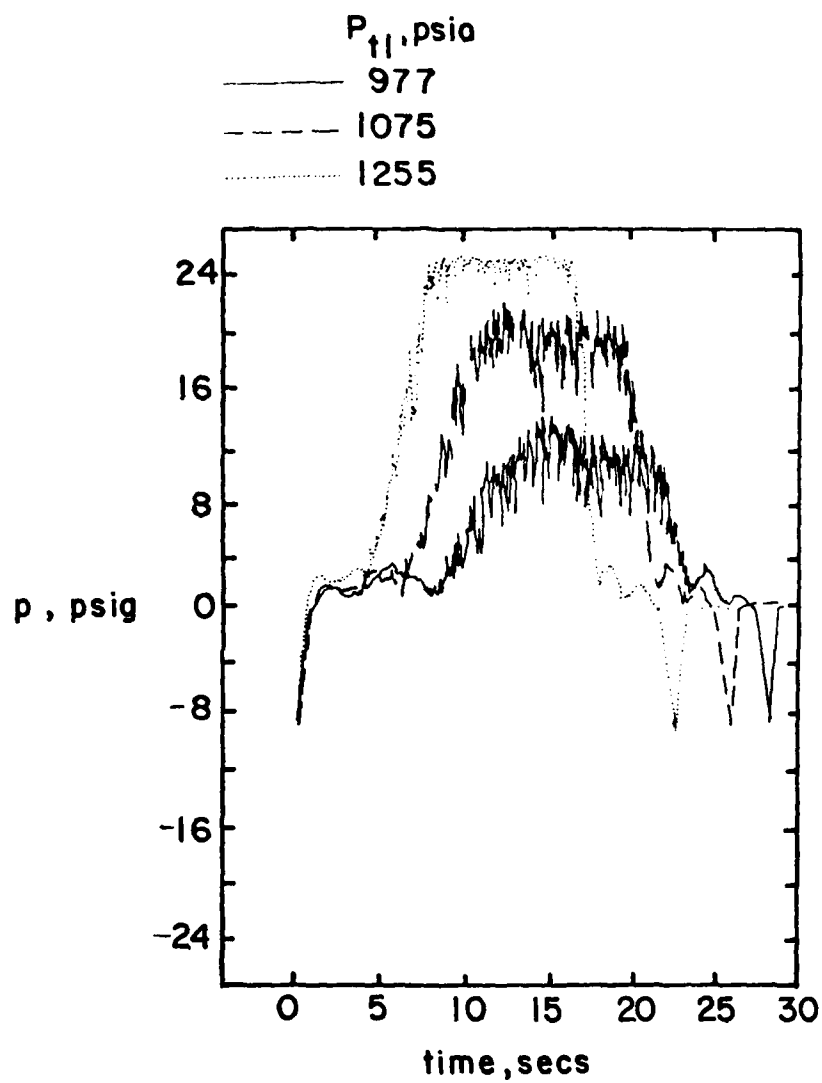
Figure 12. - Static wall-pressure measurements from the impingement region, $x_g = 0.13 \, r_{ne}$.

36

(b) Mid-range stagnation pressures.

Figure 12. - Continued.

37

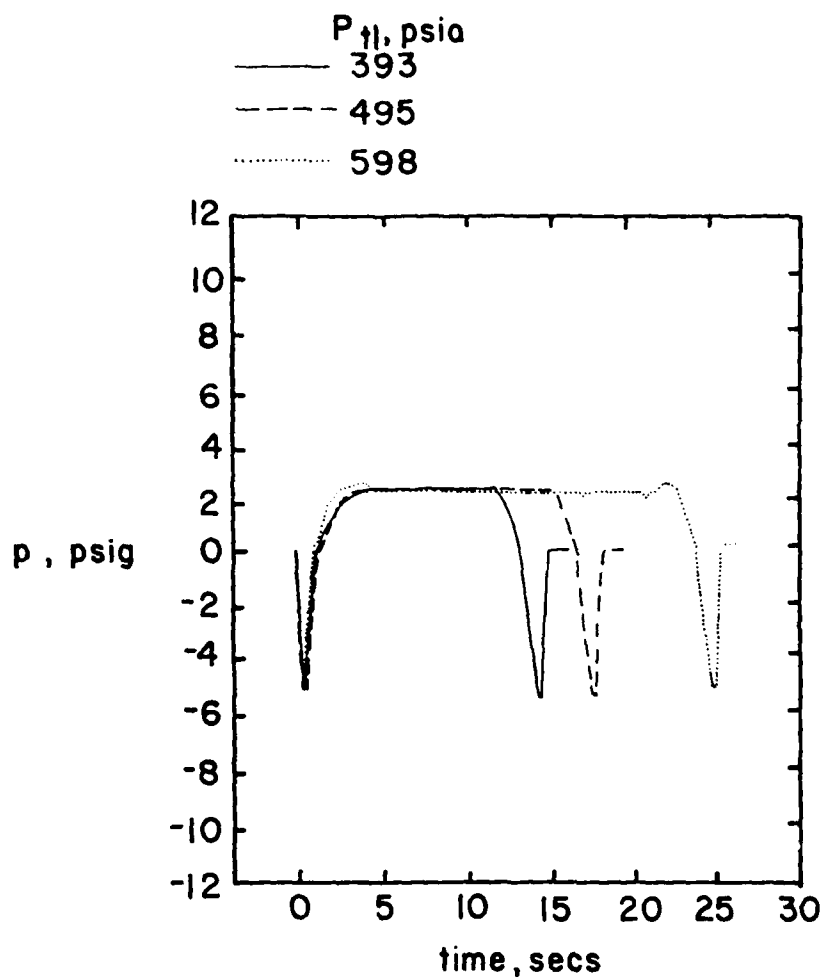(c) Relatively high stagnation pressures.

Figure 12. - Concluded.

38

Since p_{ne} is proportional to p_{t1}, the exhaust expands through a
larger angle as the stagnation pressure increases. Thus, the "location"
of the exhaust impingement on the wall moves nearer to the exit plane
as p_{t1} is increased. Furthermore, the impingement shock wave should
be stronger as the stagnation pressure increases. The wall-pressures
should also increase.

The histories for the static wall-pressures measured for
$x_g = 0.13$ r_{ne} are significantly different. These histories are
presented in Figure 12. This orifice location is, of course, nearer
to the impingement shock wave than the other two. However, it might
be noted that the gage is still upstream of the impingement point as
determined using the photograph of the free plume, which is reproduced
in the sketch of Figure 5. The fluctuating pressures at the higher
stagnation pressures, i.e., $p_{t1} \geq 880$ psia, reflect the influence
of the impinging flow from the shear layer at the plume boundary.
Note that the gage reached its maximum output for $p_{t1} = 1255$ psia.
Thus, the actual pressure was not recorded for this condition.

The wall pressures for the annular gap are presented in Figures
13 through 15. Recall that the steady-state pressures that were
presented in Figure 9 were essentially independent of position in
this region. The transient pressures also exhibit position
independence. The "steady-state" values of the static wall pressure
increase with p_{t1}. Since the blow-by flow in the annular gap
originates at the plume impingement and exhausts to the atmosphere,
it should indeed be greater than the atmospheric value. At the
higher values of p_{t1}, the pitot-pressure measurements from the
annular gap[3] indicate that the flow is nearly choked. This
explains why the corresponding pressures are well above the
atmospheric value.

[3] S. A. Bouslog and J. J. Bertin, "Flows in the Annular Region
When an Underexpanded Nozzle is exhausted into a Stepped Launch
Tube", U.S. Army Missile Command, TR RL-CR-80-4, Redstone Arsenal,
Alabama, March 1980.

P_{t1}, psia

——— 393

- - - - 495

·············· 598

p , psig

time, secs

(a) Relatively low stagnation pressures.

Figure 13. - Static wall-pressure measurements from the annular gap, $x_g = -7.19\ r_{ne}$.

40

P_{t1}, psia

———— 710

— — — 792

··········· 894
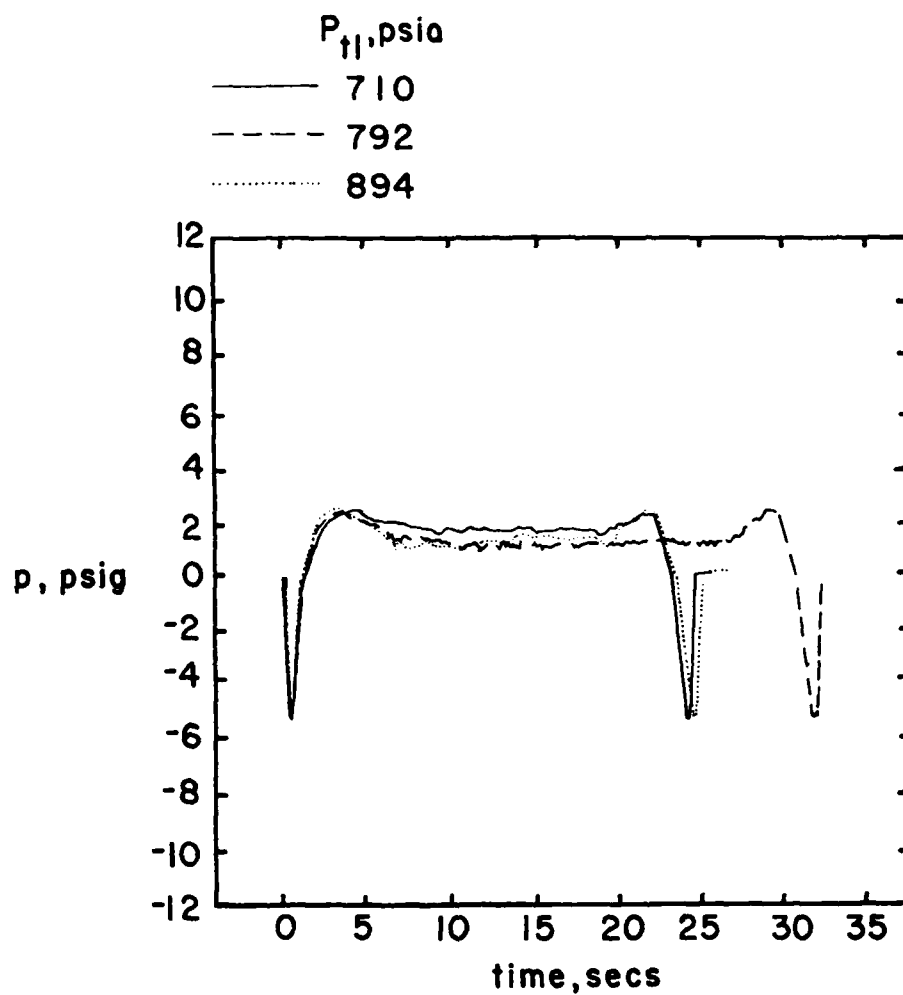
(b) Mid-range stagnation pressures.

Figure 13. - Continued.

41

(c) Relatively high stagnation pressures.

Figure 13. - Concluded.

P_{t1}, psia
——— 393
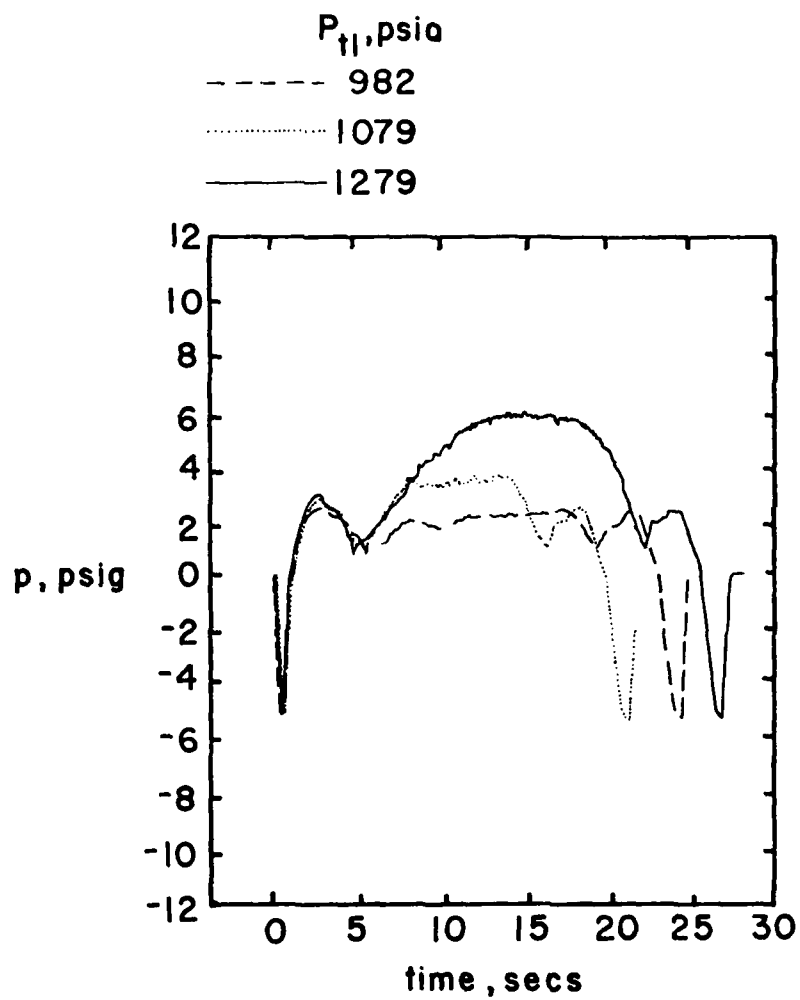·············· 491
– – – – 583

p, psig

time, secs

(a) Relatively low stagnation pressures.

Figure 14. - Static wall-pressure measurements from the annular gap, $x_g = -7.15$ r_{ne} .

43

(b) Mid-range stagnation pressures.

Figure 14. - Continued.

44

P_{t1}, psia
.... 967
----- 1089
——— 1269

(c) Relatively high stagnation pressures.

Figure 14. - Concluded.

45

P_{t1}, psia

——— 393

– – – 486

·········· 593
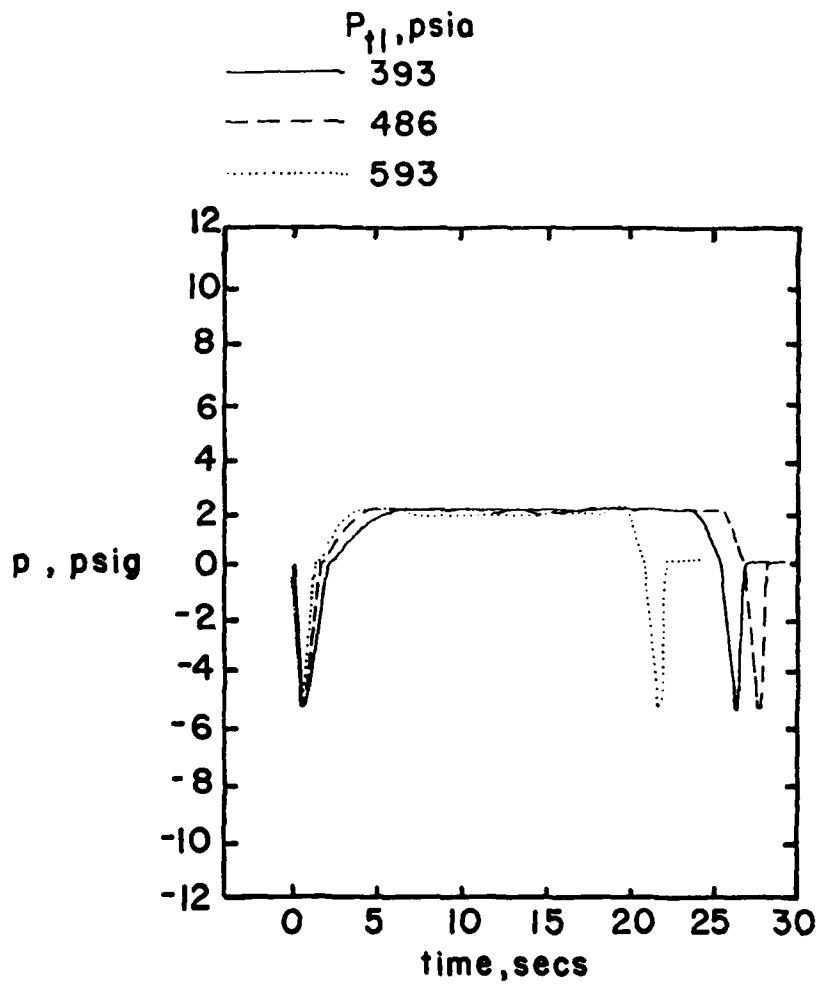
(a) Relatively low stagnation pressures.

Figure 15. - Static wall-pressure measurements from the annular gap, x_g = -7.06 r_{ne}.

46

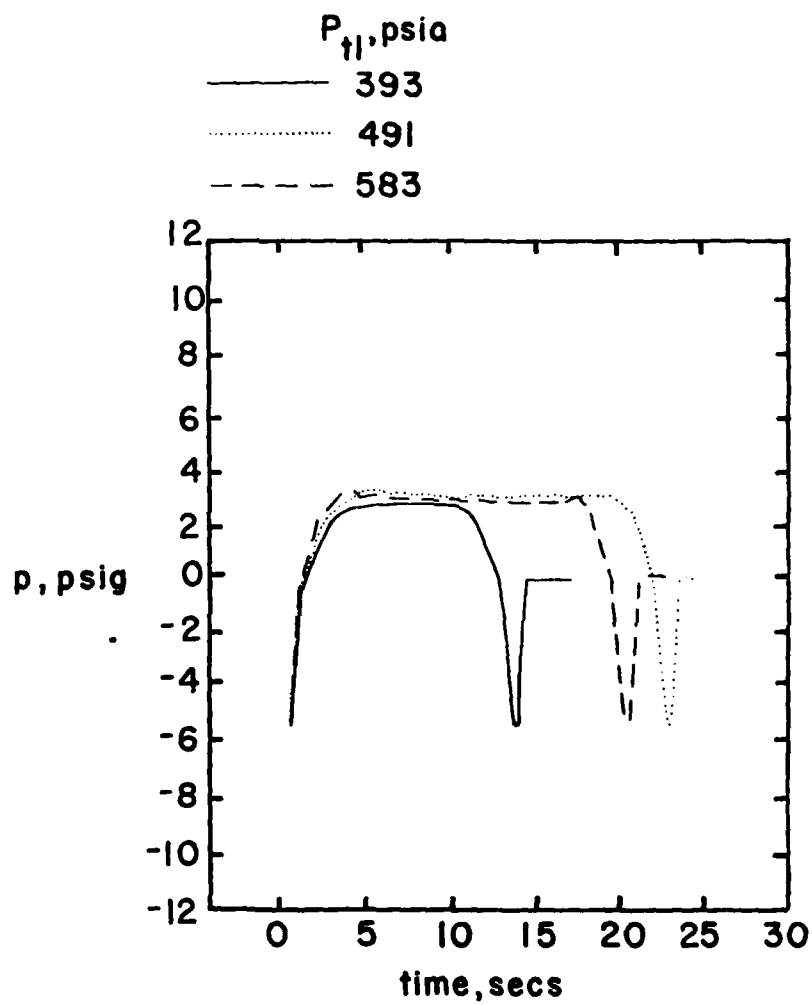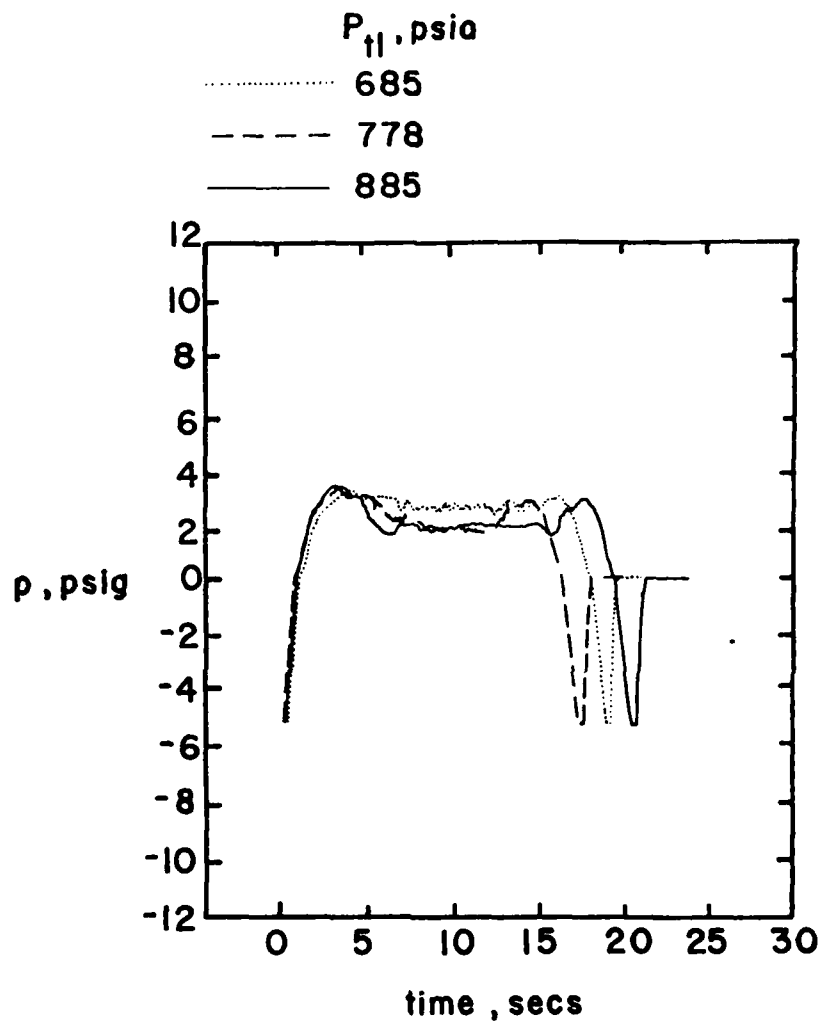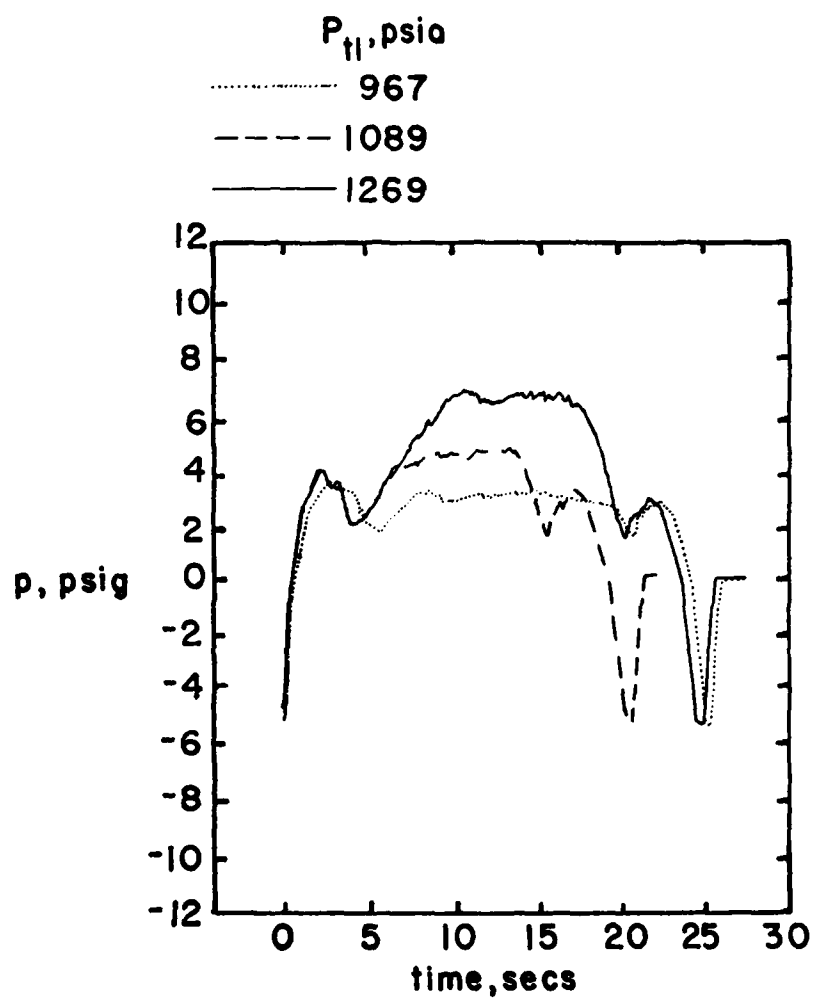P_{t1}, psia

.... 685

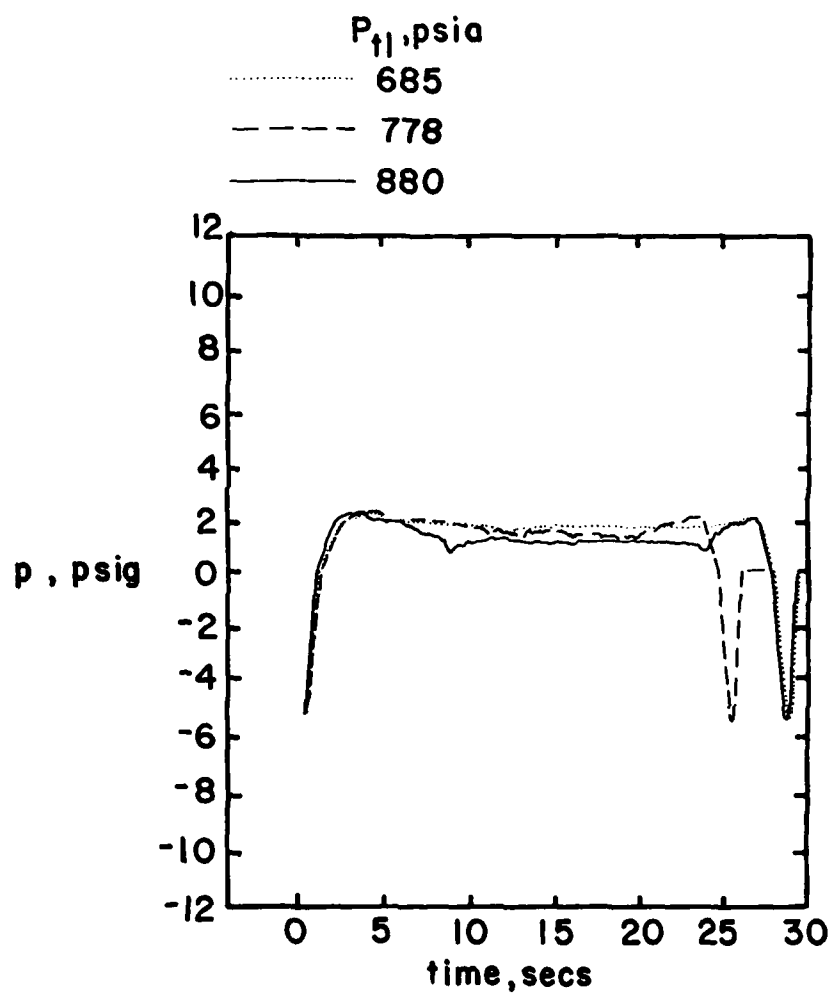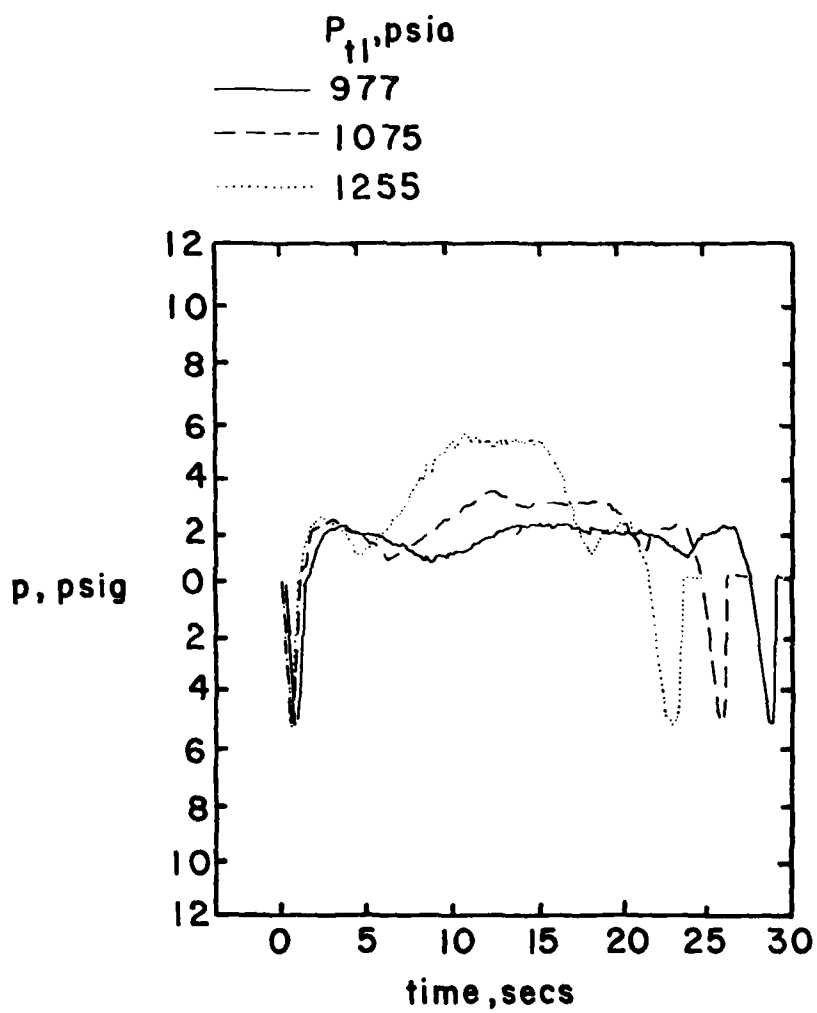− − − − − 778

───── 880

p , psig

time, secs

(b) Mid-range stagnation pressures.

Figure 15. - Continued.

47

(c) Relatively high sta[g]nation pressures.

Figure 15. - Concluded.

4. CONCLUDING REMARKS

An experimental program has been conducted using transducers
capable of measuring the unsteady pressures acting on the launcher
wall for a nozzle-exit-location of 8.0h. At this position, the
exhaust flow impinges on the launcher wall upstream of the ring but
close enough to the ring to generate significant blow-by flow. The
most interesting finding of the investigation was the transient
characteristics of the flow initiation. As the rocket motor comes
up to pressure (i.e., as the stagnation pressure increases toward its
steady-state value), large negative gage pressures exist on the wall.
Thus, at the instant of ignition, the system acts as an ejector.
Hence, because the wall pressure in this region (which serves as the
base pressure) is relatively low, the flow tends to expand through a
relatively large angle. This initial expansion angle is larger than
the "steady-state" angle. Thus, the initial impingement shock is
probably stronger than the corresponding "steady-state" condition.
The flow then "oscillates" until reaching the appropriate steady
state value. Transient behavior similar to this has been observed
in several of the flight-test programs, that have been studied by
personnel from the University of Texas at Austin.

DELIBERATELY BLANK

NOMENCLATURE

A	Cross-sectional Area
h	Radial height of constrictive ring
$\dot{m}_{ag}$	Mass flow-rate in the annular gap
$\dot{m}_{ex}$	Exhaust mass flow-rate
p	Pressure
r	Radius
x	Axial coordinate measured relative to the nozzle exit plane (see Figure 6)
$\tilde{x}$	Axial coordinate measured relative to the front face of the ring (see Figure 6)
θ	Angular measurement

Subscripts

g	Gage location
ne	Nozzle exit plane
r	External surface of the rocket
$t1$	Stagnation chamber (or reservoir) of the nozzle

Superscript

$*$	Sonic throat of the nozzle

51

DELIBERATELY BLANK

LITERATURE CITED

1. D. W. Barnette, J. J. Bertin, and J. L. Batson, "Free-Flight Rocket's Initial Trajectory as Affected by Massive Blow-by", *Journal of Spacecraft and Rockets*, Vol. 15, No. 6, Nov.-Dec. 1978, pp. 334-340.

2.   ---   : "Feasibility Flight Testing of Rocket Impelled Projectile (RIP)", Report Number 7-52100/3R-5, 1 May 1973, LTV Aerospace Corporation, Michigan Division.

3. S. A. Bouslog and J. J. Bertin, "Flows in the Annular Region When an Underexpanded Nozzle is exhausted into a Stepped Launch Tube", U.S. Army Missile Command, TR RL-CR-80-4, Redstone Arsenal, Alabama, March 1980.

4. D. R. Chapman, D. M. Kuehn, and H. K. Larson, "Investigation of Separated Flows in Supersonic and Subsonic Streams with Emphasis on the Effects of Transition", Report 1356, 1957, NACA.

5. S. J. Sutter, J. J. Bertin, D. P. Dannemiller, and E. J. Zihlman,Jr., "Study of the Exhaust Plume for Highly Underexpanded Supersonic Nozzles Exhausting into Quiescent Air", Aerospace Engineering Report 79001, January 1979, University of Texas at Austin.

6. E. S. Idar, III, J. J. Bertin, and S. Bouslog, "The Effect of Geometry on Static Wall-Pressure Distributions and Secondary Flows for Tube-Launched Rocket Configurations", Aerospace Engineering Report 79005, November 1979, *The University of Texas at Austin*.

DELIBERATELY BLANK

DISTRIBUTION

DEFENSE TECHNICAL INFORMATION CENTER
CAMERON STATION (2 COPIES)
ALEXANDRIA, VA 22314

COMMANDER
US ARMY MISSILE COMMAND
ATTN: DRSMI-O (3 COPIES)
ATTN: DRSMI-r, DR. KOBLER (1 COPY)
ATTN: DRSMI-RLH (12 COPIES)
ATTN: DRSMI-ICBB, BARBARA ROBERTS (1 COPY)
ATTN: DRSMI-RPT (2 COPIES)
ATTN: DRSMI-RDK, MR. DEEP (2 COPIES)
ATTN: DRSMI-RPR (2 COPIES)
ATTN: DRSMI-LP, MR. VOIGHT (1 COPY)
REDSTRONE ARESENAL, AL 35898

UNIVERSITY OF ILLINOIS
ATTN: DR. H. H. KORST (1 COPY)
DEPARTMENT OF MECHANICAL ENGINEERING
THE UNIVERSITY OF ILLINOIS AT URBANA-CHAMPAIGN
URBANA, ILLINOIS 61801

US ARMY MATERIAL SYSTEMS ANALYSIS ACTIVITY
ATTN: DRXSY-MP (1 COPY)
ABERDEEN PROVING GROUND, MD 21005